



## The Lustdust Property in Central British Columbia: A Polymetallic Zoned Porphyry-Skarn-Manto-Vein System

By Gerry Ray<sup>1</sup>, Ian Webster<sup>1</sup>, Peter Megaw<sup>2</sup>, Jim McGlasson<sup>2</sup> and Keith Glover<sup>3</sup>

**KEYWORDS:** *Lustdust, porphyry, skarn, manto, vein, Eocene, Cache Creek Terrane, Pinchi Fault, Takla Silver Mine, molybdenum, copper, zinc, gold, mercury, geochemistry, exploration, economic geology.*

### INTRODUCTION AND LOCATION

Alpha Gold Corporation's Lustdust property lies close to the junctions of Canyon and Silver creeks, approximately 210 km northwest of Prince George and 35 km east of Takla Lake in central British Columbia (Figure 1). It includes a skarn-manto-vein system that is discontinuously developed over a 2.5 km strike length. This mineralization is related to an elongate, undeformed, Eocene-age composite Mo-bearing porphyry body, the Glover Stock (Figure 2). The stock lies <2 km west of the Pinchi Fault (Figure 2) and it intrudes deformed oceanic rocks of the Cache Creek Terrane, including mid to Late Permian limestones. The Pinchi Fault is major north-northwest trending structure that separates the Cache Creek rocks from an intrusive suite belonging to the Quesnel Terrane immediately to the east (Gabrielse and Yorath, 1992; Figure 1).

The Lustdust area has a history of exploration and small-scale mining for Hg, Au, Ag and Zn-Pb. The former Bralorne Takla Hg mine (BC MINFILE 093N 008) lies close to the Pinchi Fault (Figure 3), and the southern part of the Lustdust property includes a developed prospect, the "Takla Silver Mine" (093N 009), which only produced some small bulk test samples. The adits at the Takla Silver Mine were driven to explore veins and carbonate replacements that represent the most southern and distal part of the Lustdust hydrothermal system. Later, it was realized that a metal zoning is present on the property; northwards, the Takla Silver Mine Ag-Pb-Au-Zn-As-Hg-bearing veins pass successively into Zn-rich mantos, Cu-Au (Zn) skarns, and then into Mo porphyry-style mineralization in the Glover Stock (Figure 2).

Previous exploration has concentrated on the more distal Zn-Ag-Au rich mantos and veins, but the economic potential of the more proximal Cu-Au skarns and Mo porphyry is now apparent. Drilling by Alpha Gold in 2000 and 2001

has been centered on these more northerly styles of mineralization.

This paper describes the geology, mineralization and alteration on the Lustdust property and outlines the proximal to distal chemical zoning in the system.

### REGIONAL GEOLOGY

The Lustdust mineralization lies in the Cache Creek Terrane (Figure 1) which represents a deformed and imbricated package of Pennsylvanian to lower Jurassic oceanic rocks (Monger 1977, 1998; Paterson, 1974, 1977; Gabrielse and Yorath, 1992). The terrane includes a western element, the Sitlika Assemblage, and an eastern portion that has been designated the Cache Creek Complex (Schiarizza and MacIntyre, 1999; Schiarizza, 2000). The latter, which host the Lustdust mineralization, includes highly deformed phyllites, argillites, cherts and thick carbonates, together with units of oceanic island basalts and mafic tuffs (Paterson, 1974, 1977; Schiarizza and MacIntyre, 1999).

During the Early to Middle Jurassic, the Cache Creek rocks were amalgamated with those of the Stikine Terrane (Figure 1) and imbrication occurred along west-directed thrust faults (Schiarizza and MacIntyre, 1999). In the Lustdust area, this probably coincided with the development of lower greenschist facies metamorphism and several periods of folding. Elsewhere in the terrane, however, some blueschist facies are locally recorded (Paterson, 1977), and these have been dated by K-Ar methods as being Late Triassic (Paterson and Harakel, 1974). Schiarizza and MacIntyre (1999) note that the most important pulses of plutonism occurred during the Middle Jurassic, Late Jurassic to Early Cretaceous and Early Cretaceous times.

The Pinchi Fault (Figure 1) can be traced for >450 km in British Columbia. It is believed to have originally formed during the Late Triassic as a major thrust related to a subduction zone that dipped northwards under Quesnellia (Paterson, 1977; Barrie, 1993). Subsequently, it was reactivated as a north-northwest trending dextral fault.

The Quesnel Terrane in this region comprises a Late Triassic volcanic-sedimentary arc succession that includes both alkalic and sub-alkalic elements. These supracrustal rocks are intruded by a number of major plutons, the largest of which is the multiphase Hogem Batholith (Figure 1). Dating by K-Ar methods (Garnett, 1978) suggests three in-

<sup>1</sup> British Columbia Ministry of Energy and Mines

<sup>2</sup> International Mineral Development & Exploration Inc.

<sup>3</sup> Consulting Geologist

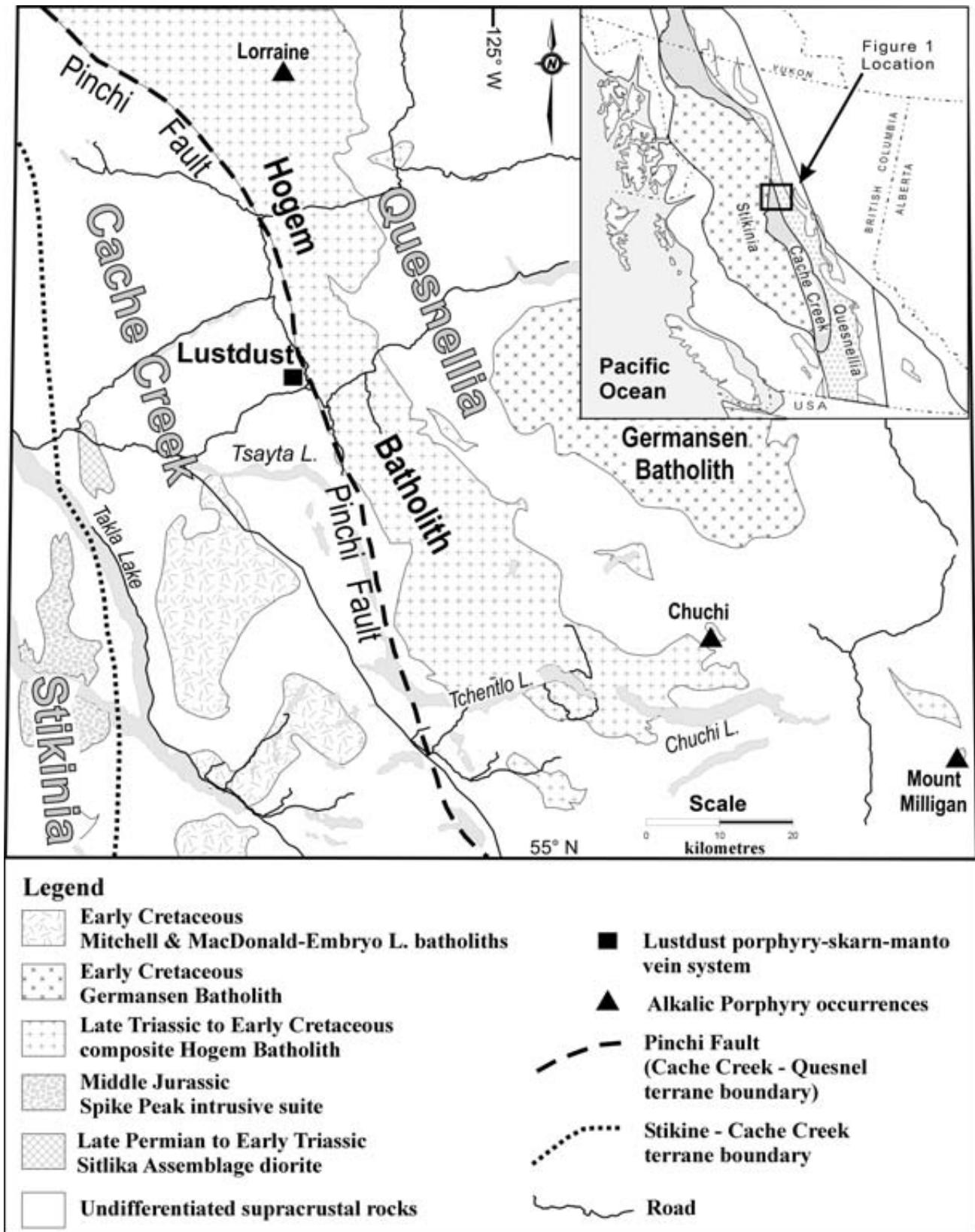


Figure 1. Map of the Takla Lake area showing the locations of the Lustdust property, the Pinchi Fault, the terrane boundaries and the major intrusions. Geology after Wheeler *et al.* (1991) and The MapPlace, October 2001.

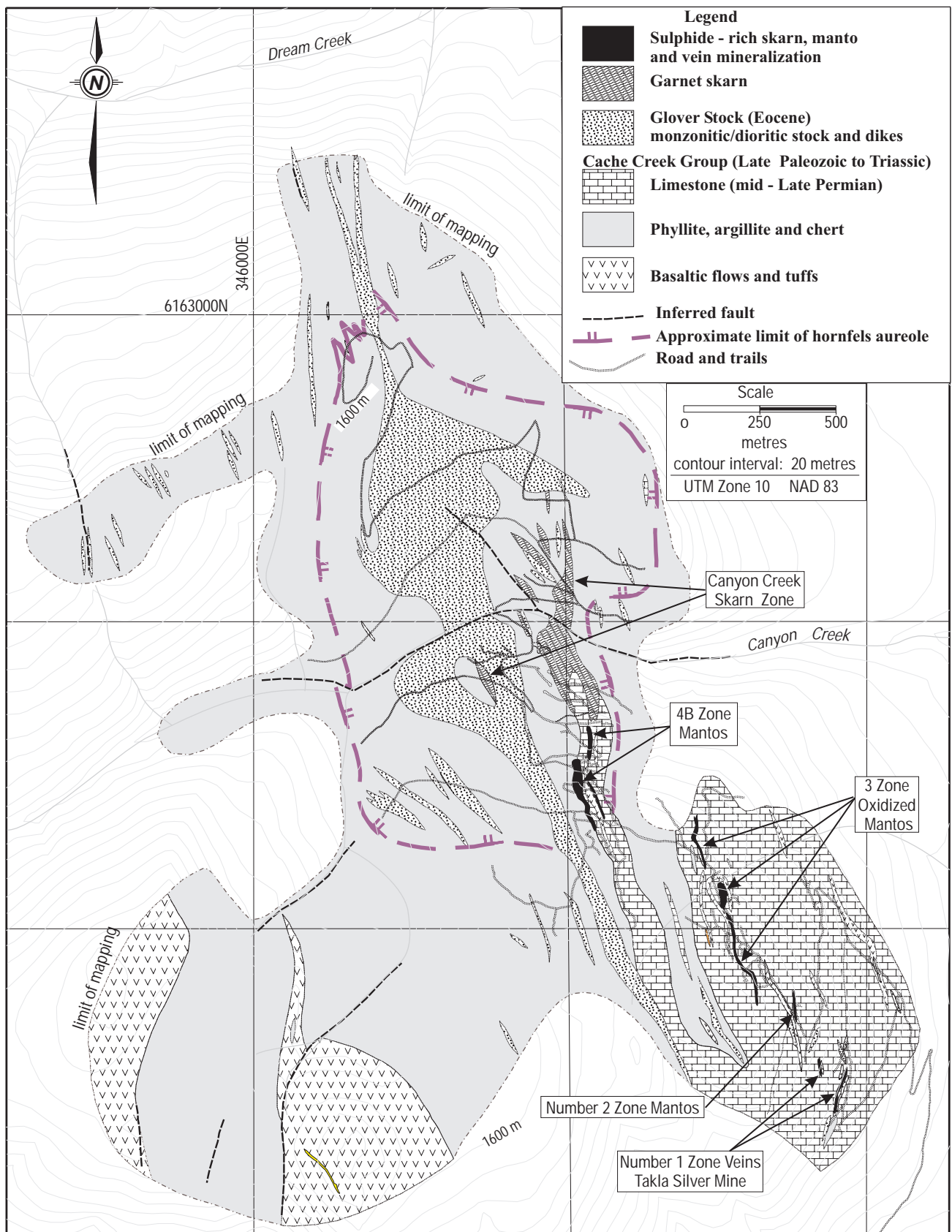


Figure 2. Geology of the Lustdust property showing location of the Glover Stock and the various proximal to distal mineralized zones. Geology compiled from mapping by Evans (1996, 1997, 1998), Megaw (1999, 2000, 2001), Glover, McGlasson, Ray and Webster (unpublished data).

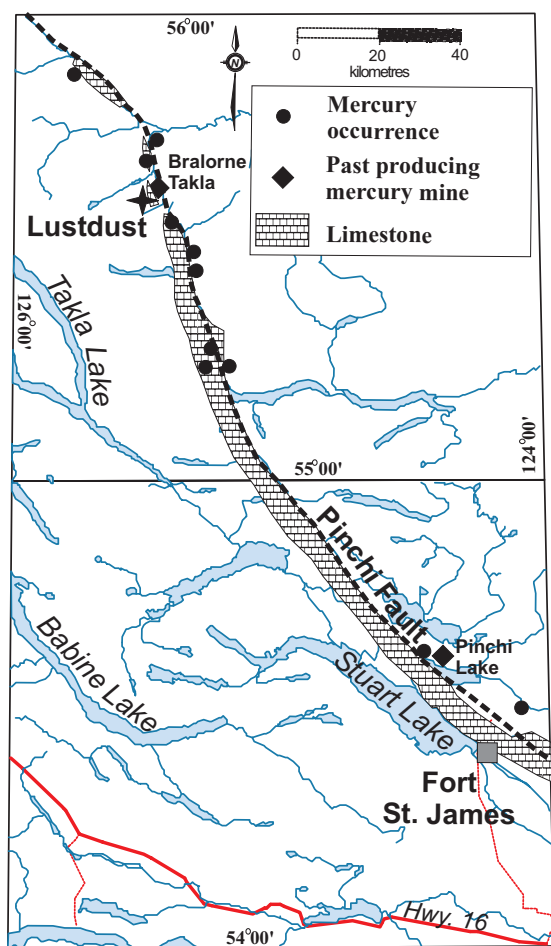


Figure 3. The Pinchi Fault north-west of Fort St. James showing prospective areas for other possible Lustdust targets associated with limestones, Hg occurrences or former Hg mines.

trusive phases, a Late Triassic to Early Jurassic suite of calc-alkaline granodiorites, a Middle Jurassic phase of alkalic syenites, and an Early Cretaceous episode of calc-alkaline granites. Porphyry Cu-Au mineralization is seen at the Lorraine, Chuchi and Mount Milligan properties (Figure 1; Bishop *et al.*, 1995). Garnett (1978) notes that much of this porphyry Cu  $\pm$  magnetite mineralization is associated with the Middle Jurassic syenites.

## PREVIOUS WORK IN THE LUSTDUST AREA

Cinnabar was discovered in 1942 on the west side of Silver Creek, along the Pinchi Fault, at what was to become the Bralorne Takla Mercury Mine (Figure 3; BC MINFILE 093N 008). Total production at the mine amounted to 59 914 kilograms of mercury during 1943 and 1944. In 1944 the Kay claims were staked on veins approximately 1.5 kilometres west of the mine on what later became the Takla Silver Mine. These Ag-Au-Pb-Zn-Hg-bearing sulphide and sulphosalt veins became known as the “Number 1 Zone” and they are now believed to be the most southerly, distal extension of the Lustdust hydrothermal system. The 1945

Minister of Mines Annual Report notes that 350 feet of underground workings had been constructed on the claim group. By 1953, the property was known as the Lustdust. Leta Explorations Ltd undertook considerable diamond drilling and development work up to 1963, and in 1960 a Noranda and Canex joint venture completed extensive trenching. In 1965, Takla Silver Mines Limited drove a new 700-foot long drift on the Number 1 Zone and also dug trenches over surface mineralization at the Number 3 Zone further north (Figure 2; Campbell, 1966). At the Number 1 Zone, Sutherland Brown (1965) reported the presence of an antimony-rich vein-like replacement in limestone and porphyry dike hostrocks. The minerals identified included stibnite, boulangerite, sphalerite, pyrite, some ruby silver and trace realgar and orpiment.

In 1968, Anchor Mines Ltd. extracted a 300-pound bulk sample from the Number 1 Zone for metallurgical testing. A mineralogical study of material taken from underground workings and surface trenches was made by Mathieu and Bruce (1970) who noted the presence of some sulphide, sulphosalt and arsenide minerals, as well as high values of Au, Ag, Pb, Zn and Sb. Zapata Granby Corporation performed geological mapping, soil sampling and geophysical surveys during 1978 and 1979. Noranda Mining and Exploration Company Limited soil sampled and mapped the area during 1979 and 1980. In 1981 they put down a number of diamond drillholes, including some on the north side of Canyon Creek. This was followed in 1986 by survey and sampling work by Welcome North Mines Ltd. and Pioneer Metals.

Alpha Gold Corporation began acquiring the property in 1991 and some exploration was undertaken (Rotzien, 1991; 1992). Later it was optioned to Teck Exploration Limited who completed an extensive exploration and drilling program (Evans, 1996, 1997). Since that time Alpha Gold has done a considerable amount of drilling that has recently focused on skarn and porphyry targets lying north and south of Canyon Creek; details on this work are summarized by Evans (1998), Soregaroli (1999) and Megaw (1999, 2000, 2001). Recently, Alpha Gold Corporation announced intersecting Mo-Cu-bearing porphyry and Cu-Au skarn mineralization along Canyon Creek (Figure 2); intersections through mineralized skarn include hole DDH01-44 which cut 59 m grading 0.8 % Cu and 0.67 g/t Au and hole DDH01-47 which cut 37 m assaying 0.92% Cu and 0.68 g/t Au (Alpha Gold Corp. News release, October 1st, 2001).

Schiarizza (2000) compiled the geology of the district, and Dunne and Ray (2002, this volume) have completed a fluid inclusion study of the Lustdust mineralization.

## GEOLOGY OF THE LUSTDUST AREA

### INTRODUCTION

The Lustdust mineralization is associated with an elongate, composite igneous body, the Glover Stock, as well as a related north-northwest-trending swarm of felsic dikes and sills (Figure 2). The stock, which crops out both north and south of Canyon Creek, intrudes deformed Cache Creek

supracrustal rocks and is surrounded by a 200 to 300 m wide hornfels aureole. The country rocks comprise a steeply west-dipping, north-northwest striking package of slaty carbonaceous or cherty argillites, phyllites, ribbon cherts and mafic metavolcanics and tuffs. Also present are several thick, north-trending units of limestone and marble that host most of the skarn, manto and vein mineralization.

## **SUPRACRUSTAL ROCKS**

Most of the Lustdust area is underlain by a north-northwest striking package of slaty phyllites and cherts, as well as lesser amounts of mafic tuff, greenstone metavolcanics and some limestones (Figure 2). In addition, there are thin, minor units of polymictic volcanic sandstone and conglomerate (Megaw, 2000). The limestones are concentrated in the southeast part of the area but quickly pinch out north of Canyon Creek (Figure 2). It is uncertain whether this northerly disappearance of the limestones in this area reflects facies changes or the northern plunge of the fold axes. Thick units of mafic volcanic and tuffaceous rocks are more common to the southwest (Figure 2), whereas the phyllitic argillites and cherts mainly occupy a north-northwest trending belt in the central portion of the property. The argillites and cherts are commonly interbedded and locally grade from one into another, making it difficult to separate and map out the two units (Figure 2). Limestones form massive to poorly bedded, fine-grained rocks that vary from blue-grey to white in color. Individual carbonate units range from a few centimeters to over 500 m in thickness. During this study, four limestone samples were collected for microfossil identification. Three of these contained no useful fossils, but one massive limestone sample (GR01-38), collected at UTM Zone 10 NAD 83 348069E - 6160847N, yielded fossils of mid to Late Permian age (M.J. Orchard, personal communication, 2001). Many limestones are sugary textured due to recrystallization (Megaw, 1999) and they contain stylolites. Adjacent to intrusive rocks, the carbonates are often bleached, silicified or converted to marble. Evans (1997) identified several different types of limestone, one of which may represent carbonate debris flows. These rocks contain knots or small boudins of white calcite which might represent recrystallized carbonate breccia clasts (Megaw, 2001). Supportive evidence for this idea is that some limestones are interbedded with, or grade into, thin units (maximum 40 m) of a distinctive green, chloritic tuff containing angular to sub-rounded clasts up to 40 cm in diameter (Photo 1). The widely scattered and matrix-supported clasts comprise mainly various types of limestone, but minor quantities of mafic to intermediate volcanics are also present (Megaw, 2000). Evans, (1997, 1999) believed these tuffaceous debris flows represented a single folded horizon. However, later work (Megaw, 1999) suggests there are several units that display considerable lateral variations, including some with graded bedding and Bouma-type sequences. Evans (1996, 1999) reports that these tuffs locally contains up to 2% finely disseminated pyrite-pyrrhotite and are geochemically anomalous in Pb, Zn and Cu.

The most extensive area of mafic metavolcanic and tuffaceous rocks outcrops in the southwest part of the mapped area (Figure 2). All of these rocks are highly chloritized and many of the original igneous or depositional textures have been destroyed. Unlike the thin tuffaceous units interbedded with limestone further east, no brecciated limestone clasts are seen in these rocks. The volcanoclastic rocks are mostly fine-grained and massive and are believed to represent deformed and altered basaltic ash tuffs. Occasionally they contain small lithic fragments and lapilli, and in some outcrops a weak to moderate layering or sedimentary bedding is observed (*e.g.* at UTM 346476E - 6160321N). Locally, the tuffs include thin horizons of thinly bedded tuffaceous siltstone. The metavolcanic rocks are generally fine grained and massive, but at UTM 346151E - 6160757N, remnant pillow structures are observed.

The phyllites are believed to represent weakly metamorphosed argillites. They make up non-calcareous, massive to thin bedded rocks that vary from light grey to black in colour. Many outcrops contain variable quantities of carbonaceous material as well as pyrite-pyrrhotite that occurs either as disseminations or in thin beds; Megaw (2000, 2001) suggests the latter may indicate syn-sedimentary sulphide deposition. Many of the phyllites are strongly deformed and the original bedding has been transposed and obliterated. In some localities, however, intersections between the bedding and the phyllitic cleavage are recognizable.

Many of the phyllites are cherty and locally these pass into massive or well-bedded ribbon cherts that are white to very dark grey in colour. The ribbon cherts often comprise 1 to 3 cm thick layers of pale chert that are interbedded with thinner (0.25 to 1 cm) horizons of dark phyllite.

## **INTRUSIVE ROCKS**

The Lustdust mineralization is spatially associated with the Glover Stock and a related swarm of felsic sills and dikes that exceeds 3.5 km in strike length (Figure 2; Megaw, 2001). The stock crops out north and south of Canyon Creek and forms an elongate, north-northwest-trending lens-like body whose main portion exceeds 1 km in length and 0.6 km in width. It is enveloped by a 100 to 300 m wide thermal aureole which includes a biotite-dominant hornfels and lesser amounts of calc-silicate and pyroxene-bearing hornfels. Fine-grained, calc-silicate skarnoid overprints the carbonates while the purple-brown coloured biotite hornfels is developed in the argillites and argillitic ribbon cherts. There is a mineral zoning in the hornfels with biotite tending to form more distally and pyroxene occurring more proximal to the stock. The pyroxene hornfels locally includes abundant fine-grained pyrite and pyrrhotite (Megaw, 2001).

To the north and south, the Glover Stock passes out into a series of narrow, north-northwest-striking porphyritic dikes and sills. These elongate minor bodies tend to be more leucocratic and quartz-bearing than the main stock, and some have been classified as "felsites" (Megaw, 2001). Many are feldspar porphyritic but, unlike the main stock, they generally lack significant hornfels development in the wall rocks.

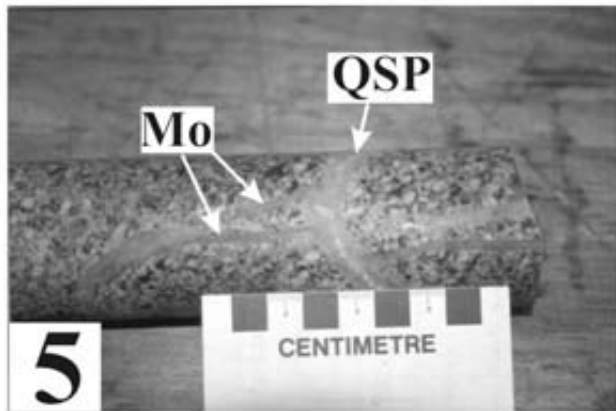
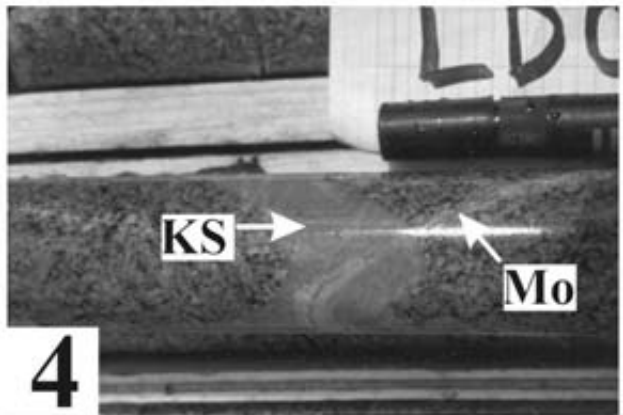
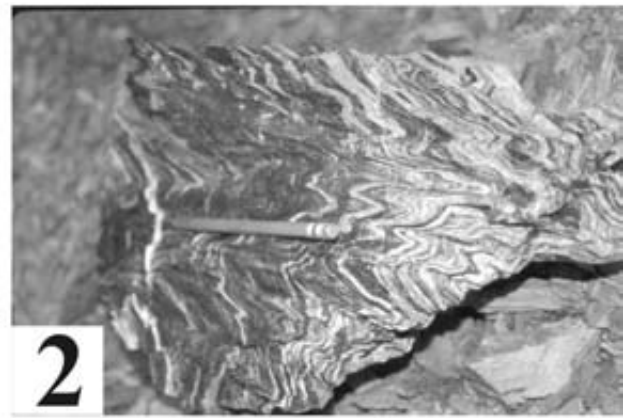
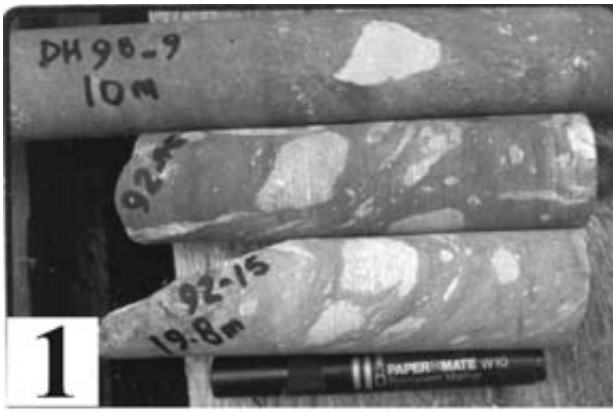


Photo 1. Mafic tuff containing clasts of limestone and minor amounts of mafic volcanic rocks. Holes LD 98-9 and 92-15 at 10 m and 19.8 m respectively.

Photo 2. Argillites, strongly deformed by open to tight F2 folds. Float located 5.2 km southwest of the Takla Silver Mine, UTM 344400E - 6156398N.

Photo 3. Hornfelsed argillitic ribbon cherts cut by early pink, barren quartz-K feldspar veins. Hole LD01-36 at 233 ft. These early veins cut both the Glover Stock (*see* Photo 4) and the hornfels envelope.

Photo 4. Glover Stock porphyry. Early, pink, quartz-K feldspar vein (KS) cut by a thin vein (Mo) containing quartz, molybdenite and trace chalcopyrite. Hole LD01-34 at 436 ft.

Photo 5. Glover Stock porphyry. Two veins (Mo) containing quartz, molybdenite and pyrite cut and displaced by a younger quartz-sericite-pyrite vein (QSP). Hole LD01-34 at 233 feet.

Photo 6. Dioritic Glover Stock cut by a vein with a quartz-feldspar-pyrite core and tourmaline-rich margins. Note the thin bleached and altered zone adjacent to the vein. Hole LD01-30 at 145 ft.

Preliminary U-Pb dating of zircons extracted from both the dioritic and monzonitic phases of the Glover Stock yield Eocene ages of circa 51 to 52 Ma (R. Friedman, personal communication, 2001). The stock represents a multiphase composite intrusive complex, and most of its rocks are weakly to strongly feldspar porphyritic; some of the latter have “crowded” feldspar porphyry textures, in addition to phenocrysts of igneous hornblende and biotite. Chemical plots (Tables 1A and 1B; Figure 4) and thin section studies (Leitch, 2001b, personal communication) indicate the stock ranges compositionally from mafic diorite-monzodiorite to more leucocratic monzonite-quartz monzonite. The age relationships between these phases is complex as the diorites both cut, and are cut by the more leucocratic igneous rocks.

Primary mafic minerals in the dioritic phases include up to 20 % hornblende with lesser biotite and rare relict clinopyroxene. The hornblende is commonly partially to totally replaced by chlorite, actinolite and secondary biotite. Primary igneous biotite comprises up to 5 % and is also chloritized. Phenocrysts of andesine-oligoclase plagioclase may exceed 60 % of the rock and individual crystals reach 3 mm in length. Potassium feldspar, both as megacrysts and small crystals in the fine-grained groundmass, may reach 15 % by volume, but is generally less than 5 %. Groundmass quartz rarely exceeds 10 %. Other accessory to trace minerals identified in the diorites includes calcite, sphene, apatite, zircon and up to 2 % opaque minerals which mainly constitute magnetite (Leitch, 2001b).

The leucocratic monzonitic phases contain 30 to 35 % plagioclase, up to 35 % K feldspar, and between 5 and 10 % quartz. Locally, some of these rocks are megacrystic with K feldspar phenocrysts up to 0.8 cm in length. Leitch (2001b) has identified relict hornblende and biotite crystals which are now replaced by aggregates of carbonate, chlorite, sphene and opaque minerals. Where intense phyllic alteration has taken place, fine grained pervasive sericite may make up 10 % of the rock and this mineral is seen replacing the plagioclase crystals. Sphene may also be replaced by sericite in addition to chlorite, and minute needles of rutile. Accessory and trace minerals in the monzonites include magnetite, apatite, zircon and pyrrhotite (Leitch, 2001b).

Thin (< 1 metre) zones of hydrothermal breccia cut the stock in some localities and many have “pebble” breccia textures. One 20 cm thick breccia zone seen in hole LD 01-36 at 186 feet contains subangular to subrounded fragments up to 3 cm across. The fragments are mostly altered diorite with lesser amounts of mafic volcanics, vein quartz and massive pyrite, that are supported in a fine-grained feldspathic matrix.

Whole rock and trace element analyses of the Glover Stock are listed in Tables 1A and 1B and plots of these data shown in Figure 4. These show that the stock represents a metaluminous, volcanic arc granitoid (Figure 4G, H and O), as defined by Pearce *et al.* (1984). The ferric and ferrous Fe content of the mafic and leucocratic phases indicate the rocks are relatively oxidized, which is typical for plutons associated with Cu skarns (Figure 4M and N). However, plots do indicate significant differences between the more mafic dioritic phases and the leucocratic monzonites which is re-

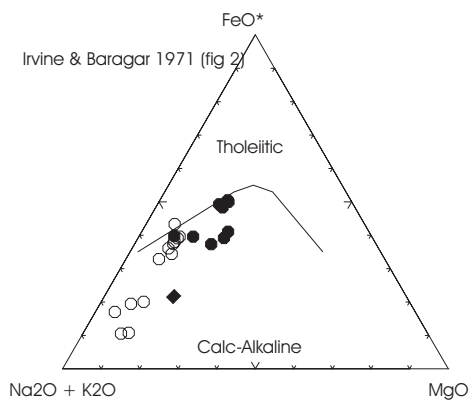
flected in their Na, K and Ba contents (Figure 4K and L). The mafic phases are subalkaline, calc-alkaline rocks of diorite-quartz diorite-monzodiorite composition while the leucocratic samples have alkalic affinities, being of monzonite-quartz monzonite-monzodiorite composition (Figure 4A to 4F). The alkalic feature is probably due to secondary potassic (K feldspar, sericite and biotite) and albitic hydrothermal alteration, as suggested by plots in Figure 4K and 4L.

Figure 5 presents comparative chondrite normalized rare earth element (REE) plots for the Hogem Batholith (Barrie, 1993) and the mafic and felsic phases of the Glover Stock. These two phases have virtually identical REE patterns, which indicates their common source. However, the pattern for the Hogem Batholith differs, notably in being comparatively depleted in light REE's (Figure 5). At the start of this project, the Glover Stock was thought to be related to the nearby Hogem Batholith (Figure 1). However, the Eocene age of the stock and its different REE pattern (Figure 5) prove it is not part of the Hogem suite.

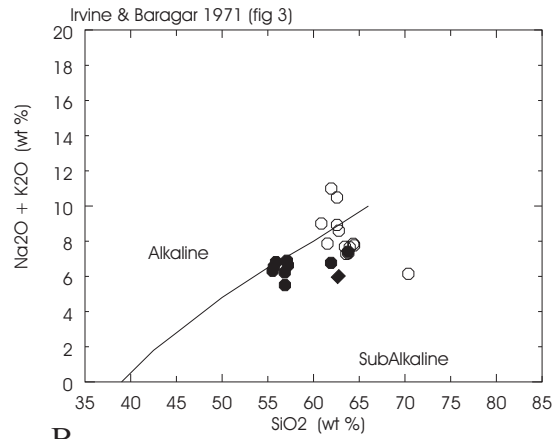
## **STRUCTURE AND METAMORPHISM**

The supracrustal rocks in the Lustdust area have undergone a complex history of brittle-ductile deformation that was probably related to both the Jurassic-age accretion of the Cache Creek Group onto the North American continent and later recurrent dextral transcurrent movements along the Pinchi structure. Two phases of deformation are recognized at Lustdust and these correspond with the two main episodes identified in Cache Creek rocks by Paterson (1974, 1977). The earliest of these (D1) was the dominant folding event and was largely responsible for the general north-northwest strike of the supracrustal rocks. It resulted in tight to isoclinal asymmetric F1 folds accompanied by a lower greenschist facies metamorphism and the development of chlorite-sericite-actinolite axial planar phyllitic S1 cleavages. These cleavages are common in the phyllites and ribbon cherts but are absent or less well developed in the more massive cherts, volcanics and limestones. Due to the absence of bedding in many rocks, small scale, outcrop-sized F1 folds are not commonly seen. However, changes in bedding-S1 intersections indicate the presence of relatively large-scale F1 structures in some localities. The F1 folds have steeply west dipping, north-northwest-trending axial planes and their fold axes plunge north to northwest, generally at between 10 and 50 degrees.

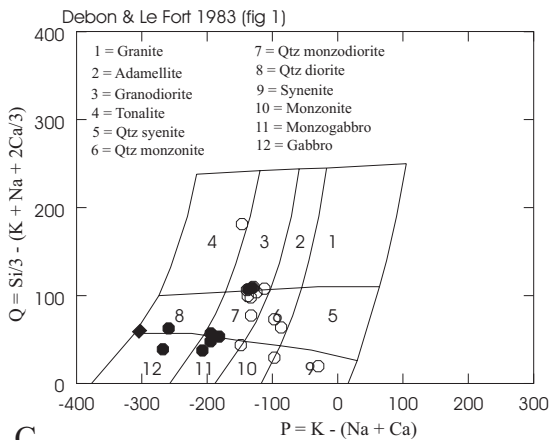
The second phase of deformation (D2) resulted in a variety of structures that vary from tight to open flexure folds (Photo 2) as well as a crenulation strain-slip cleavage in the phyllitic rocks. In some localities, two conjugate sets of strain slip cleavage are developed. The F2 folds have a wide variation of strike and plunge, depending on the orientation of the bedding and S1 surfaces. The most common F2 folds have northerly striking axial planes and fold axes that dip between 20 and 75 degrees north-northeast to northwest. The less common set strikes easterly with shallow (<15 degrees) east to west plunging axes. Locally, the F2 folds are also associated with prominent a-c joints that are often



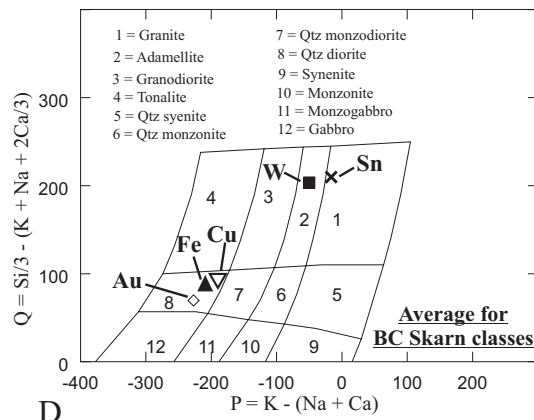
A



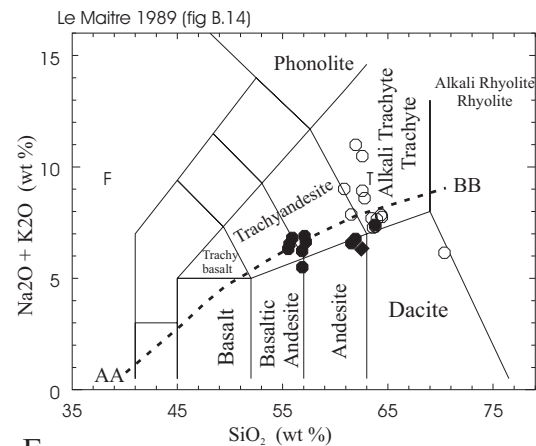
B



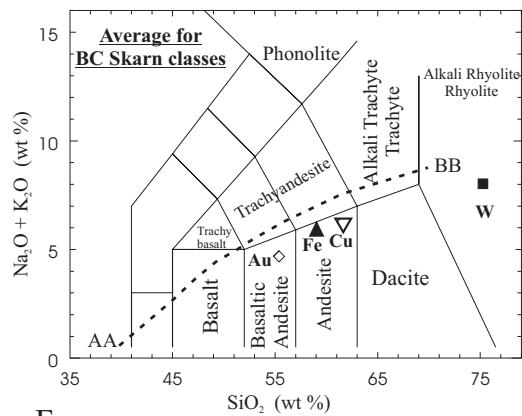
C



D



E



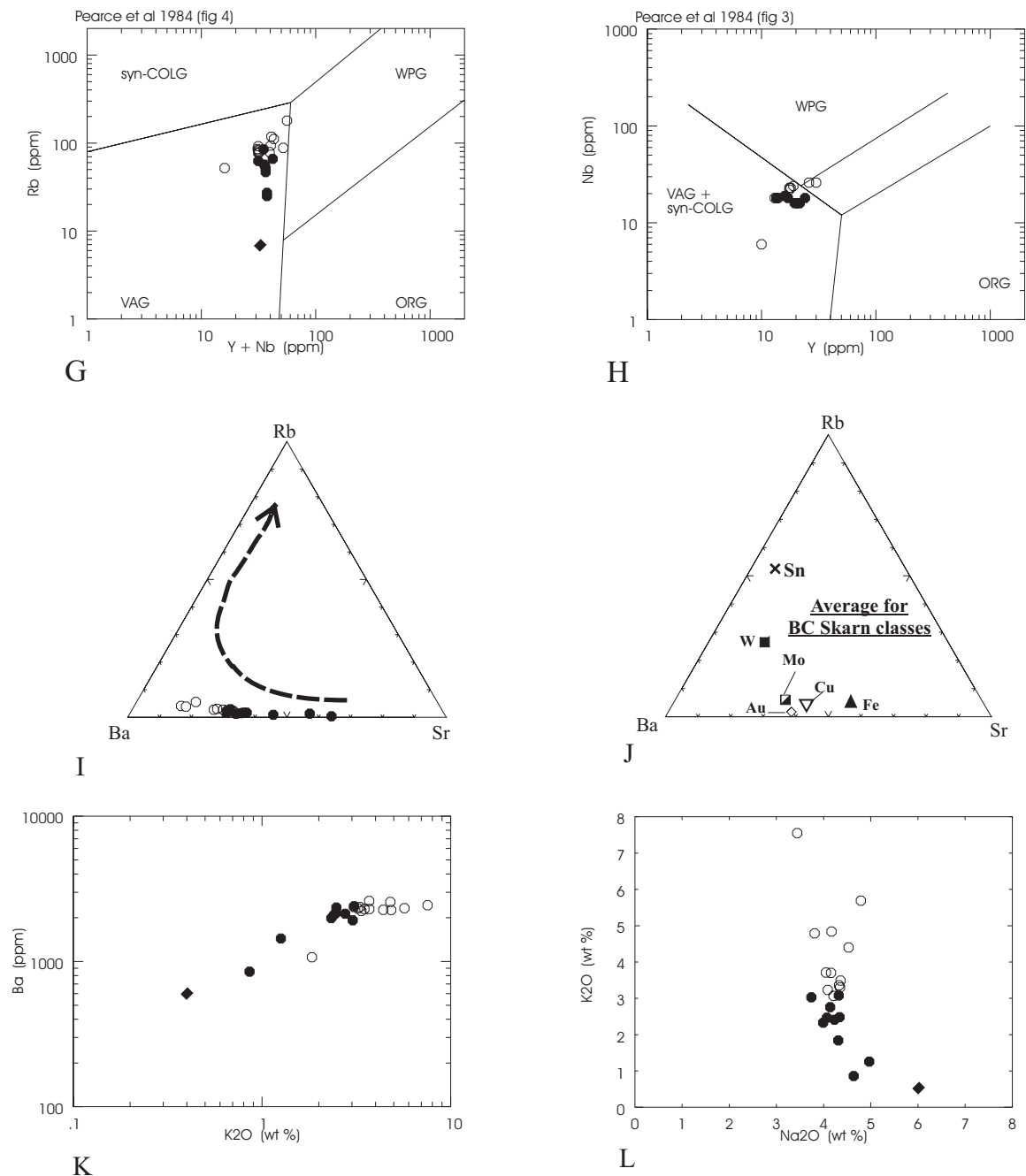
F

### Mean values for other skarn-related intrusions in B.C.

- ◇ Au skarn-related intrusions (n = 27)
- ▲ Fe skarn-related intrusions (n = 49)
- ▽ Cu skarn-related intrusions (n = 59)
- W skarn-related intrusions (n = 21)
- × Sn skarn-related intrusions (n = 19)

- Glover Stock mapped as “diorite”
- Glover Stock mapped as “monzonite”
- ◆ Albitized diorite

Figure 4.

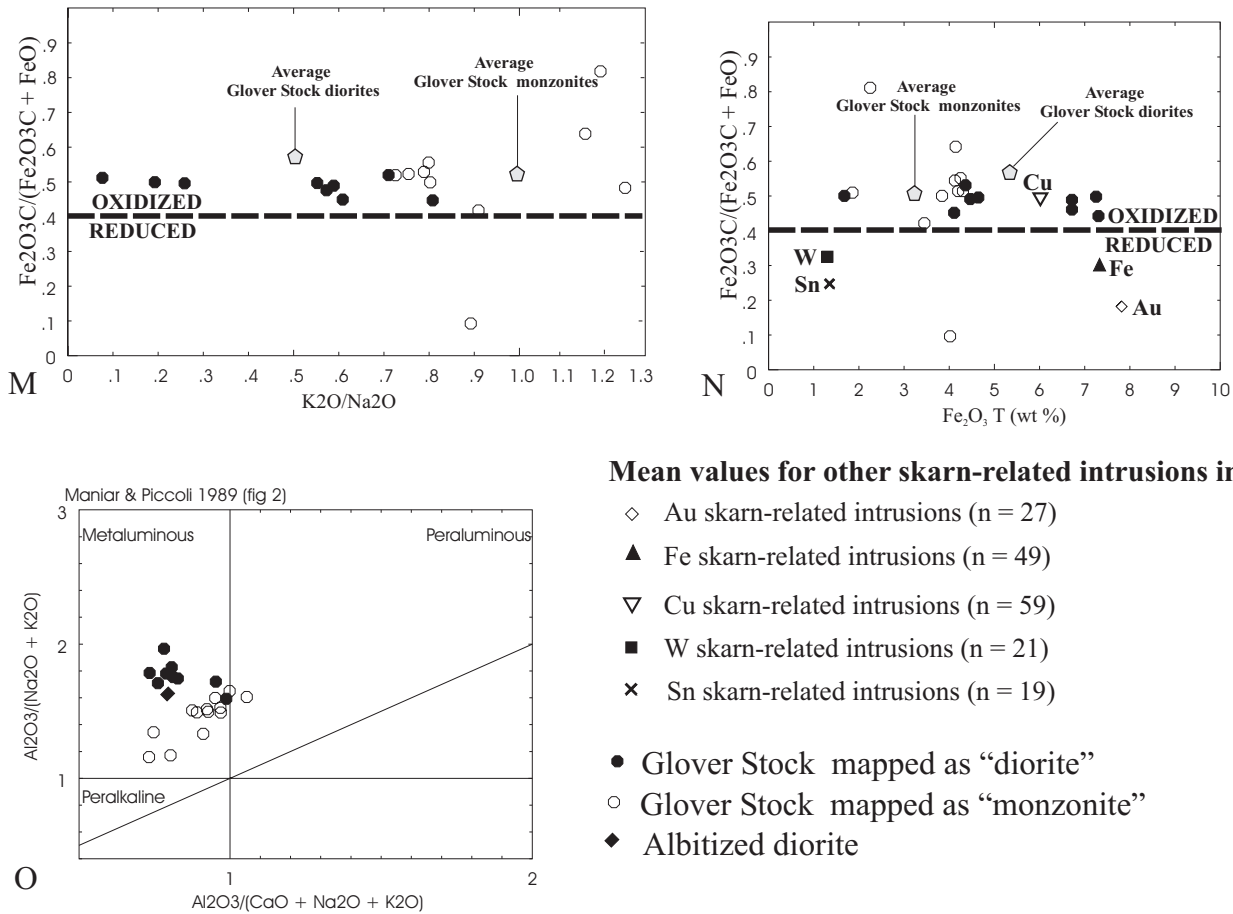


- Glover Stock mapped as “diorite”
- Glover Stock mapped as “monzonite”
- ◆ Albitized diorite

**Mean values for other skarn-related intrusions in B.C.**

- ◇ Au skarn-related intrusions (n = 27)
- ▲ Fe skarn-related intrusions (n = 49)
- ▽ Cu skarn-related intrusions (n = 59)
- W skarn-related intrusions (n = 21)
- × Sn skarn-related intrusions (n = 19)
- ▣ Mo skarn-related intrusions (n = 12)

Figure 4.



### Mean values for other skarn-related intrusions in B.C.

- ◇ Au skarn-related intrusions (n = 27)
  - ▲ Fe skarn-related intrusions (n = 49)
  - ▽ Cu skarn-related intrusions (n = 59)
  - W skarn-related intrusions (n = 21)
  - × Sn skarn-related intrusions (n = 19)
- Glover Stock mapped as “diorite”
  - Glover Stock mapped as “monzonite”
  - ◆ Albitized diorite

Figure 4. Major and trace element plots of the mafic dioritic and leucocratic monzonitic phases of the Glover Stock (data from Tables 1A and 1B). Also plotted, for comparison, are the average values of other skarn-related plutons in BC (data from Ray and Webster, 1997). A and B: AFM and alkali-silica plots (after Irvine and Baragar, 1971). C and D: Q - P plots (after Debon and Le Fort, 1983). E and F: Alkali versus silica plots (after Le Maitre *et al.*, 1989). Line AA-BB represent alkaline-subalkaline line in Figure 4B. G and H: Log Rb versus Log Y+Nb tectonic discrimination plots (after Pearce *et al.*, 1984). I and J: Triangular Ba-Rb- Sr plots (arrow is typical differentiation trend). K: Ba versus  $\text{K}_2\text{O}$  plot. L:  $\text{K}_2\text{O}$  versus  $\text{Na}_2\text{O}$  plot. M: Calculated  $\text{Fe}_2\text{O}_3\text{C}/(\text{calculated } \text{Fe}_2\text{O}_3 + \text{FeO})$  versus  $\text{K}_2\text{O}/\text{Na}_2\text{O}$  (oxidized-reduced line after Meinert, 1995). N: Calculated  $\text{Fe}_2\text{O}_3\text{C}/(\text{calculated } \text{Fe}_2\text{O}_3 + \text{FeO})$  versus total Fe as  $\text{Fe}_2\text{O}_3$ . O: Aluminum saturation plot (after Maniar and Piccolli, 1989).

spaced from 1 to 15 cm apart. These a-c joints usually strike easterly and dip northerly at between 10 and 75 degrees.

Much of the intense brittle faulting predates the emplacement of the Glover Stock and has been an important control on the mineralization. However, drilling has identified some faults that post-date the mineralization (Megaw, 2000, 2001). Most faults trend north-northwest, sub-parallel to the dominant strike of the supracrustal and intrusive rocks (Figure 2). A less common set, which may be controlled by the F2 a-c jointing, strikes east to east-northeast, and is best developed along Canyon Creek (Figure 2).

## MINERALIZATION AND ALTERATION

### INTRODUCTION

The Lustdust mineralization can be discontinuously traced for over 2.5 km, from Glover Stock porphyry-style mineralization in the north, to the quartz-sulphide-sulphosalt-bearing Number 1 Zone veins at the former Takla Silver Mine in the south (Figure 2). Limestone and marble along the eastern flank of the stock host the Cu-Au (Zn)-bearing Canyon Creek skarn which passes southwards into massive sphalerite-dominant mantos and carbonate replacements of the 2, 3 and 4B zones (Figure 2). The most southerly mineralization comprises a series of narrow, en echelon, polymetallic veins comprising the Number 1 Zone. These veins probably represent the most distal part of the

**TABLE 1A**  
**WHOLE ROCK AND TRACE ELEMENT ANALYTICAL DATA OF LEUCOCRATIC, MONZONITE SAMPLES,**  
**GLOVER STOCK, LUSTDUST PROPERTY**

Sample	GR01-16	GR01-17	GR01-45	GR01-52	GR01-55	GR01-59	GR01-63	GR01-95	GR01-96	GR01-97	GR00-28	GR00-29	GR00-30	Average
Al2O3	17.08	16.45	16.34	16.32	16.38	16.28	16.87	16.26	16.11	16.1	14.59	16.41	16.02	16.25
CaO	4.25	3.55	4.31	3.24	3.84	3.38	3.67	3.78	3.07	3.63	2.61	5.37	4.43	3.78
Fe2O3T	1.84	2.14	4.01	3.77	4.27	3.38	4.24	4.14	4.08	4.09	1.84	1.38	1.62	3.14
K2O	4.79	5.69	3.7	3.49	3.07	3.71	3.23	3.3	4.84	3.36	1.84	4.4	7.55	4.07
MgO	1.37	0.68	1.18	1.36	1.55	1.58	1.49	1.47	1.32	1.46	0.68	1.36	1.37	1.30
MnO	0.06	0.05	0.08	0.04	0.06	0.05	0.07	0.06	0.04	0.05	0.04	0.07	0.07	0.06
Na2O	3.81	4.79	4.16	4.36	4.21	4.05	4.09	4.35	4.17	4.33	4.31	4.53	3.44	4.20
P2O5	0.23	0.22	0.28	0.27	0.31	0.33	0.31	0.28	0.3	0.32	0.09	0.27	0.29	0.27
SiO2	62.78	62.57	61.53	64.35	63.6	64.44	63.82	63.96	60.85	63.45	70.39	62.58	61.94	63.56
TiO2	0.58	0.58	0.65	0.58	0.59	0.59	0.64	0.59	0.69	0.6	0.21	0.58	0.56	0.57
LOI	2.34	2.74	2.93	1.1	1.16	1.36	0.81	0.82	2.5	1.33	2.22	2.13	1.41	1.76
Sum	99.13	99.46	99.17	98.88	99.04	99.15	99.24	99.01	97.97	98.72	98.82	99.08	98.70	98.95
FeO	0.85	0.37	3.3	1.8	1.94	1.86	1.84	1.88	1.39	1.8	NA	NA	NA	1.70
Fe2O3C	0.90	1.73	0.34	1.77	2.11	1.31	2.20	2.05	2.54	2.09	1.84	1.38	1.62	1.25
Fe2O3C/ (Fe2O3C+FeO)	0.51	0.82	0.09	0.50	0.52	0.41	0.54	0.52	0.65	0.54	NA	NA	NA	0.51
K/Na	1.26	1.19	0.89	0.80	0.73	0.92	0.79	0.76	1.16	0.78	0.43	0.97	2.19	0.99
Ba	2570	2330	2610	2300	2370	2300	2320	2370	2260	2230	1070	2270	2440	2264.62
Rb	111	118	93.4	82.8	76.8	91.8	77.8	80.6	78.8	85.4	52	88	180	93.57
Sr	971	423	1250	1065	1050	961	1055	1060	1105	993	220	814	600	889.77
Nb	24	23	23	18	18	18	18	18	22	18	6	26	26	19.85
Zr	269	253	254	203	178	187.5	185.5	177	220	169	90	210	204	200.00
Y	19	18	17.5	13.5	13.5	13.5	14	13.5	17.5	13	10	26	30	16.85
Ce	133	134.5	131.5	98	92.5	91	95.5	94	123.5	92.5	NA	NA	NA	108.60
Co	3	3.5	7	6	6	5.5	4.5	5.5	4.5	7.5	NA	NA	NA	5.30
Cs	1.4	2	1.8	1.9	1.9	2.1	1.4	1.8	1.6	2	NA	NA	NA	1.79
Cu	15	45	40	130	55	190	85	90	410	360	NA	NA	NA	142.00
Dy	3.9	4	3.7	2.6	2.6	2.7	3	3	3.7	2.8	NA	NA	NA	3.20
Er	1.7	1.6	1.6	1.3	1.3	1.4	1.3	1.4	1.8	1.3	NA	NA	NA	1.47
Eu	2	1.9	1.9	1.3	1.6	1.5	1.4	1.5	1.7	1.4	NA	NA	NA	1.62
Ga	20	21	21	20	19	19	19	20	21	20	NA	NA	NA	20.00
Gd	5.8	6.2	5.5	4.7	4.5	4.3	4.3	4.5	5.7	4.3	NA	NA	NA	4.98
Hf	6	6	5	4	4	4	4	4	5	4	NA	NA	NA	4.60
Ho	0.6	0.6	0.6	0.5	0.4	0.5	0.4	0.5	0.6	0.4	NA	NA	NA	0.51
La	58.5	59.5	58.5	45	43	41.5	43.5	43.5	55	41.5	NA	NA	NA	48.95
Lu	0.3	0.3	0.2	0.1	0.1	0.2	0.1	0.1	0.3	0.2	NA	NA	NA	0.19
Nd	49	48	47.5	35.5	34.5	33	33.5	35	45.5	33.5	NA	NA	NA	39.50
Ni	30	25	10	<5	<5	<5	<5	<5	<5	15	NA	NA	NA	20.00
Pb	20	10	20	25	30	15	20	20	15	25	NA	NA	NA	20.00
Pr	13.9	14.2	13.9	10.2	10	9.5	9.9	9.9	13.2	9.3	NA	NA	NA	11.40
Sm	7.8	7.8	7.9	5.7	5.4	5.4	5.3	5.8	7.2	5.3	NA	NA	NA	6.36
Sn	1	2	1	<1	1	<1	<1	<1	1	1	NA	NA	NA	1.17
Ta	0.5	0.5	0.5	0.5	0.5	0.5	0.5	0.5	0.5	0.5	NA	NA	NA	0.50
Tb	0.8	0.8	0.8	0.6	0.6	0.6	0.5	0.6	0.7	0.6	NA	NA	NA	0.66
Th	15	15	14	12	12	12	13	14	14	13	NA	NA	NA	13.40
Tl	0.5	0.5	1.5	0.5	0.5	0.5	0.5	0.5	0.5	1	NA	NA	NA	0.65
Tm	0.3	0.3	0.2	0.1	0.1	0.1	0.2	0.1	0.2	0.1	NA	NA	NA	0.17
U	6.5	5	6	5.5	6	6.5	5.5	6	6	6	NA	NA	NA	5.90
V	65	65	75	70	75	85	105	80	85	80	NA	NA	NA	78.50
W	<1	2	1	<1	<1	4	<1	<1	<1	3	NA	NA	NA	2.50
Yb	1.9	1.7	1.5	1.1	1.1	1.2	1.3	1.5	1.6	1.3	NA	NA	NA	1.42
Zn	115	15	30	400	55	25	30	25	15	40	NA	NA	NA	75.00

Analyses completed by ALS Chemex, 212 Brookbank Ave, Vancouver, BC  
Major elements in percent; other elements in ppm; NA = sample not analyzed for the element  
Major elements except FeO by XRF  
FeO by HCl-HF digestion & titrimetric finish  
Ba, Nb, Rb, Y and Zr by XRF  
Other elements by lithium meta-borate fusion and ICP-MS

Sample description and location

	UTM	UTM
GR01-16	346939	6162113 LD01-32, 340 ft chlorite-epidote altered crowded feldspar porphyry dike
GR01-17	346939	6162113 LD01-32, 349 ft crowded feldspar porphyry dike with moderate pyrite-sericite alteration
GR01-45	347080	6161207 LD93-7, 9.5m pale altered monzonite with 2% disseminated pyrite, altered hornblende and hydrothermal biotite
GR01-52	346495	6162132 LD01-34, 724 ft, monzonite
GR01-55	346495	6162132 LD01-34, 347 ft monzonite with some K-spar alteration
GR01-59	346495	6162132 LD01-34, 200 ft monzonite with minor pyrite
GR01-63	346495	6162132 LD01-34, 388 ft hornblende monzonite
GR01-95	346495	6162132 LD01-34, 392 ft. hornblende monzonite w pinkish feldspar crystals up to 0.5 cm
GR01-96	346495	6162132 LD01-34, 399 ft. Medium grained hornblende monzonite
GR01-97	346495	6162132 LD01-34, 181 ft. Coarse grained hornblende monzonite with trace disseminated pyrite
GR00-28	346888	6161077 Narrow dike of light grey feldspathic monzonite
GR00-29	346950	6161770 DH20-25, 575 ft, Weakly altered crowded feldspar porphyry ?monzonite
GR00-30	347005	6161740 DH20-05, 415 ft, Megacrystic crowded feldspar ?monzonite. Moderate bleaching

**TABLE 1B**  
**WHOLE ROCK AND TRACE ELEMENT ANALYTICAL DATA OF MAFIC, DIORITIC SAMPLES,**  
**GLOVER STOCK, LUSTDUST PROPERTY**

SAMPLE	GR01-69	GR01-70	GR01-71	GR01-72	GR01-73	GR01-74	GR01-86	GR01-107	GR01-108	GR00-27	Average
Al2O3	16.78	16.69	17.03	16.6	16.84	17.57	16.23	16.79	16.63	17.09	16.83
CaO	6.72	6.49	7.52	6.32	7.14	6.88	4.18	6.11	3.52	5.98	6.09
Fe2O3T	6.85	7.24	4.62	7.26	4.48	1.67	4.09	6.79	4.28	6.69	5.40
K2O	2.48	2.47	1.26	2.33	0.86	0.42	3.03	2.41	3.08	2.76	2.11
MgO	3.44	3.7	3.6	3.48	3.38	1.97	2.06	3.06	1.32	3.21	2.92
MnO	0.12	0.11	0.08	0.09	0.08	0.04	0.04	0.1	0.05	0.13	0.08
Na2O	4.34	4.07	4.97	3.99	4.64	6.08	3.74	4.23	4.32	4.14	4.45
P2O5	0.61	0.62	0.63	0.59	0.57	0.43	0.43	0.56	0.3	0.46	0.52
SiO2	55.91	55.66	56.85	55.54	56.88	62.4	61.93	57.2	63.79	57.09	58.33
TiO2	0.97	1	0.97	0.95	0.93	0.75	0.77	0.91	0.57	0.85	0.87
LOI	0.65	1.18	1.51	1.86	3.05	1.18	2.48	0.85	1.05	0.19	1.40
TOTAL	98.87	99.23	99.04	99.01	98.85	99.39	98.98	99.01	98.91	98.59	98.99
FeO	3.43	3.72	2.18	3.45	2.16	0.76	2.1	3.31	1.9	NA	2.56
Fe2O3C	3.03	3.10	2.19	3.42	2.08	0.82	1.75	3.11	2.17		2.55
Fe2O3C/ (Fe2O3C+FeO)	0.47	0.45	0.50	0.50	0.49	0.52	0.45	0.48	0.53	NA	0.57
K/Na	0.57	0.61	0.25	0.58	0.19	0.07	0.81	0.57	0.71	0.67	0.50
Ba	2350	2160	1440	1985	851	611	1920	2100	2400	2130	1794.70
Rb	46.6	51.4	25	54.6	27.2	6.8	84.8	56.8	62.4	66	48.16
Sr	1200	1180	1210	1175	1140	1090	893	1190	1065	948	1109.10
Nb	16	16	16	16	16	18	19	16	18	18	16.90
Zr	196	182	189	192.5	198	206	182.5	181.5	194.5	162	188.40
Y	20.5	20.5	21.5	20	21.5	17	16	19.5	13.5	24	19.40
Ce	104	102.5	93.5	99.5	106.5	98.5	106	102	93	NA	100.61
Co	11.5	15.5	22	13.5	9	0.5	8	12	7	NA	11.00
Cs	1.2	1.8	0.9	2.8	2	0.5	4.9	3	0.8	NA	1.99
Cu	25	20	50	35	45	55	195	60	85	NA	63.33
Dy	4	4.4	4.4	4.3	4	3.2	3	4.1	3	NA	3.82
Er	2.1	2	2.2	2	2	1.7	1.5	1.8	1.2	NA	1.83
Eu	2.1	2	1.9	2	2	1.7	1.6	2	1.5	NA	1.87
Ga	21	21	20	21	20	21	19	21	21	NA	20.56
Gd	6.1	6.3	6.4	6.5	6.1	5.3	5	6	4.4	NA	5.79
Hf	4	4	4	4	4	4	4	4	4	NA	4.00
Ho	0.7	0.7	0.8	0.7	0.8	0.6	0.5	0.7	0.5	NA	0.67
La	43.5	43	37.5	43	47.5	43.5	47.5	43.5	42	NA	43.44
Lu	0.3	0.3	0.3	0.3	0.3	0.2	0.2	0.3	0.1	NA	0.26
Nd	45	42	41.5	41.5	44	39	39	41.5	34	NA	40.83
Ni	<5	<5	5	<5	<5	<5	<5	5	<5	NA	5.00
Pb	10	15	15	20	15	20	20	20	20	NA	17.22
Pr	11.8	11.4	10.8	11	11.5	10.7	11.3	11.2	10	NA	11.08
Sm	7.3	7.6	7.9	7.4	7.6	6.8	6.3	7.1	5.4	NA	7.04
Sn	<1	1	2	1	3	3	1	1	1	NA	1.63
Ta	<0.5	<0.5	<0.5	<0.5	<0.5	0.5	<0.5	<0.5	0.5	NA	0.50
Tb	0.8	0.8	0.9	0.9	0.9	0.6	0.7	0.8	0.6	NA	0.78
Th	9	8	8	8	9	12	9	10	12	NA	9.44
Ti	<0.5	0.5	<0.5	0.5	0.5	<0.5	0.5	<0.5	0.5	NA	0.50
Tm	0.3	0.3	0.3	0.2	0.3	0.2	0.3	0.3	0.1	NA	0.26
U	3	3	4	3	4.5	4.5	4	3	7	NA	4.00
V	145	150	155	160	160	100	95	140	75	NA	131.11
W	<1	<1	3	1	3	1	6	3	<1	NA	2.83
Yb	1.9	1.8	2.2	1.7	2.1	1.7	1.4	1.8	1.1	NA	1.74
Zn	65	75	55	85	50	100	40	70	35	NA	63.89

Analyses completed by ALS Chemex, 212 Brookbank Ave, Vancouver, BC  
Major elements in percent; other elements in ppm; NA = sample not analyzed for the element  
Major elements except FeO by XRF  
FeO by HCl-HF digestion & titrimetric finish  
Ba, Nb, Rb, Y and Zr by XRF  
Other elements by lithium meta-borate fusion and ICP-MS

Sample locations & descriptions

	UTM	UTM	
GR01-69	346484	6161771	LD01-30, 395 ft weakly altered hornblende-biotite diorite with 15 % mafics
GR01-70	346484	6161771	LD01-30, 382 ft unaltered diorite
GR01-71	346484	6161771	LD01-30, 397 ft bleached & altered hornblende-biotite diorite
GR01-72	346484	6161771	LD01-30, 350 ft dark hornblende-biotite diorite, moderately chloritized. Some hairline pyrite veinlets
GR01-73	346484	6161771	LD01-30, 356 ft dark hornblende-biotite diorite, moderately chloritized. Some hairline pyrite veinlets
GR01-74	346484	6161771	LD01-30, 847 ft bleached, albitized and, chloritized monzonite with Mo-bearing veinlets
GR01-86	346448	6162051	LD01-36, 327 ft, grey, wkly porphyritic hornblende-biotite diorite. Moderate alteration & disseminated pyrite
GR01-107	346484	6161771	LD01-30, 134 to 150 ft. Unaltered hornblende diorite
GR01-108	346342	6162469	LD01-39, 467-547 ft. Biotite-hornblende diorite with trace pyrite veinlets
GR00-27	347003	6162467	Dark diorite with 8-10 % biotite-hornblende phenocrysts. Pyrite on fractures

Lustdust hydrothermal system; alternatively, they may represent high sulphidation mineralization that formed above another buried intrusion emplaced south of the Glover Stock (see Figure 9, Dunne and Ray, 2002, this volume).

Megaw (2001) notes that the manto and vein mineralization is strongly controlled by (1) the presence of carbonate hostrocks, (2) lithological contacts including dike and sill margins or limestone-tuff contacts, (3) bedding planes and faults, and (4) antiformal fold hinges.

Lustdust represents a classic intrusion-related system that exhibits distinct proximal to distal zoning, both in its mineralogy and metal chemistry (Evans, 1996; 1998; Megaw, 1999, 2000, 2001). Changes in the chemistry and estimated formation temperatures of the fluid inclusions throughout the system also reflect this zonation (Dunne and Ray, 2002, this volume). Outboard from the porphyry, Megaw (2001) notes that much of the mineralized belt is auriferous (>0.5 g/t Au). Assay data for the various styles of mineralization are shown in Tables 2A to 2E and the average values of the elements and metal ratios are presented in Table 3.

### **PORPHYRY MINERALIZATION IN THE GLOVER STOCK**

The Glover Stock, which outcrops north and south of Canyon Creek, hosts molybdenite ± chalcopyrite-bearing veinlets with classic porphyry-style alteration selvages. This mineralization is developed in both the dioritic and monzonitic phases; the best intersection are in drillhole LD01-39 which cut an 8.8m wide zone with 0.24 % Mo (Megaw, 2001). Mineralization is often associated with several generations of either barren or mineralized veins containing variable amounts of quartz, K feldspar, sericite, pyrite and rare tourmaline. Assay values on some of the mineralization are presented in Table 2A, and Megaw (2001) notes the following styles of porphyry-related alteration:

1. Tourmaline related to quartz veins that cut the diorite south of Canyon Creek. The tourmaline may occur in the veins (Photo 6), or as replacements of the diorite adjacent to the vein margins.
2. Early, generally barren K feldspar-quartz veins cut the stock (Photo 4) and also extend out into the hornfels (Photo 3).
3. Potassic alteration that includes: (a) secondary biotite selvages on mineralized veinlets, (b) secondary euhedral and/or “shreddy” biotite replacing primary biotite and hornblende, (c) secondary pervasive K feldspar flooding and (d) weak to strong pervasive sericitic alteration of the intrusions.
3. Widespread late chloritization and epidotization of the igneous hornblendes and feldspars.

Porphyry-style mineralization in the Glover Stock includes:

1. Quartz-tourmaline veins containing minor pyrite and chalcopyrite (Photo 6).
2. Quartz-K feldspar-pyrite-chalcopyrite veinlets.

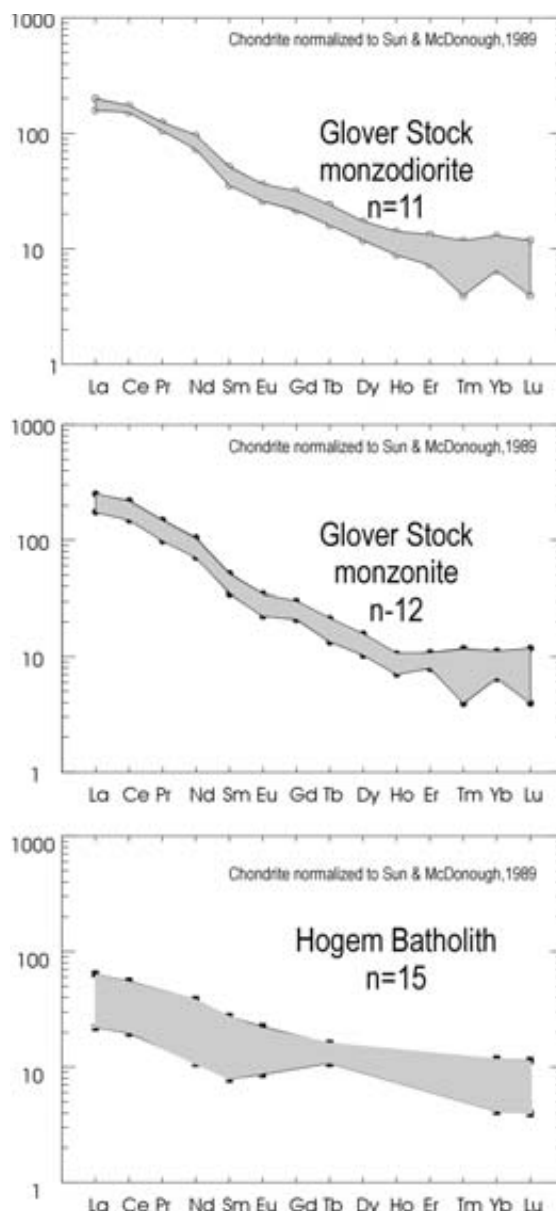


Figure 5. Comparative chondrite normalized rare earth element (REE) plots of the maximum and minimum element ranges (ppm) for the Hogem Batholith and the mafic dioritic and leucocratic monzonitic phases of the Glover Stock. Hogem Batholith data from Barrie (1993). Note the Light Rare Earth Element (LREE) enrichment in the Glover Stock relative to the Hogem Batholith.

3. Quartz-K feldspar-pyrite-molybdenite veinlets (Photos 4 and 5).
4. Younger quartz-K feldspar ± pyrite veinlets that cut the Mo-bearing veins (Photo 5).
5. Igneous hornblendes that are replaced, in turn, by specularite and then magnetite containing interstitial chalcopyrite.
6. Open sigmoidal cavities lined with early quartz-K feldspar-pyrite and then filled with specularite, epidote and rare, late garnet.

**TABLE 2A**  
**ASSAY DATA OF GLOVER STOCK PORPHYRY SAMPLES, LUSTDUST PROPERTY**

No.	IWE01-2	GR01-50	GR01-51	GR01-53	GR01-58
Ag	0.2	0.4	0.36	0.6	0.42
As	50	66.2	64.6	9.6	5
Au	4	6	2	9	4
Bi	0.4	0.7	0.2	1.1	0.3
Cd	<0.20	6.98	2.1	10.45	2.66
Ce	98	91.5	83.2	78.9	72.6
Co	7	3.5	3.4	6.9	6.2
Cr	90	112	57	177	97
Cu	119.2	80	46.8	165.9	117.1
F	450	660	910	780	740
Fe	3.09	1.2	1.08	1.99	1.38
Ga	22	15.15	19.4	18.55	15.8
Ge	<0.50	0.2	0.2	0.2	0.15
Hg	<10	10	<10	<10	<10
In	0.05	0.09	0.025	0.125	0.03
K	2.41	2.7	3.03	2.57	2.13
La	55	56	50.5	46	43.5
Mg	1.06	0.48	0.71	0.62	0.6
Mn	600	90	120	135	135
Mo	5.5	201	362	866	899
Na	3.08	2.17	2.32	2.24	2.07
Nb	22	10	11.7	12.5	10.4
Ni	16	4.8	4	6.2	5.4
P	1700	1030	970	990	900
Pb	65	15	13.5	51.5	10.5
S	<0.10	0.71	0.35	1.12	0.74
Sb	52	6.95	4.9	45.85	3.4
Se	<10	<1	<1	1	1
Sn	<2.0	0.6	0.8	0.8	0.8
Te	<0.50	0.2	0.05	0.5	0.25
Tl	1	0.86	0.9	0.78	0.9
U	3	4.1	4.7	4.5	3.9
W	1	8.8	2.5	2.4	2.9
Zn	120	708	134	838	38

Analytical methods etc., for Tables 2A - 2F.  
Analyses performed at ALS Chemex, 212 Brooksbank Avenue, North Vancouver, B.C. V7J 2C1  
Au by fire assay and Induced Coupled Plasma-Mass Spectrometry (ICP-MS); reported in ppb  
F by carbonate nitrate fusion and specific ion electrode finish; reported in ppm  
All other elements analyzed by combined ICP-MS and ICP-Atomic Emission Spectroscopy. Hg & Au reported in ppb  
Fe, K, Mg, Na and S reported in per cent. All other elements in ppm. <= below detection limit.  
Note: ICP-MS detections levels were raised for some samples to reflect high-grade sulphide analysis.  
Locations using NAD 83, UTM Zone 10 co-ordinates.  
Sample descriptions & locations:  
IWE01-2: Sub-crop of hornblende-biotite monzonite with pyrite and trace chalcopyrite. 346428E 6162162N  
GR01-50: LD01-34; 559 feet. Coarse grained monzonite with disseminations and veinlets of pyrite and trace molybdenite. 346495E 6162133N  
GR01-51: LD01-34; 540 feet. Coarse grained monzonite with disseminations and veinlets of pyrite-molybdenite. 346495E 6162133N  
GR01-53: LD01-34; 456 feet. Monzonite with molybdenite-quartz-pyrite veins and trace chalcopyrite. 346495E 6162133N  
GR01-58: LD01-34; 221 feet. Monzonite cut by quartz-pyrite-molybdenite veinlets. 346495E 6162133N

The paragenesis of the porphyry Mo mineralization is:

1. Quartz-tourmaline-pyrite ± chalcopyrite (early pre-mineralization).
2. Quartz-K feldspar-pyrite-chalcopyrite (early mineralization phase).
3. Quartz-pyrite-molybdenite-chalcopyrite-bornite (main mineralization phase).
4. Quartz-sericite-pyrite-chalcopyrite (late mineralization phase).
5. Quartz-pyrite (post-mineralization).

### **CANYON CREEK SKARN**

The Canyon Creek skarn (Megaw, 1999) forms a north-trending, garnet-dominant body that mostly lies east of the Glover Stock (Figure 2). It is usually hosted by limestones but has also replaced argillite, hornfels and clastic tuff, as well as some intrusive rocks to produce endoskarn. Garnet is the most abundant prograde mineral; it may exceed 80 % of the skarn and forms coarse-grained, euhedral

crystals that reach 1 cm in diameter. Clinopyroxene is far less common, forming between 0 and 15 % by volume and occurring as small (<0.25 mm) euhedral to subhedral crystals. Where later hydrous alteration has taken place, the relict clinopyroxene is extensively corroded and partially replaced by fine-grained chlorite, carbonate and possible hydrobiotite (Leitch, 2001a). Other retrograde minerals include up to 20 % calcite, 10 % quartz, and variable quantities of amphibole, biotite and chlorite (Leitch, 2001a). Minor amounts of epidote, vesuvianite and wollastonite have also been seen, the latter tending to occur along the outermost contact between garnet skarn and marble.

In surface outcrop, the garnets mostly form pale yellow-green to pale greenish brown crystals, but locally they are cut by younger veins of dark brown garnet. Megaw (1999, 2001) notes that the younger, darker, and presumably more Fe-rich garnet becomes dominant with depth. In thin section, the pale garnets occur as highly fractured, euhedral to subhedral crystals that have a distinctive yellow-green colour (Leitch, 2001a). They exhibit minor anomalous anisotropism and prominent zoning that is partly due to the

**TABLE 2B**  
**ASSAY DATA OF CANYON CREEK SKARN SAMPLES, LUSTDUST PROPERTY**

No.	GR01-9	GR01-20	GR01-22	GR01-23	GR01-24	GR01-28	GR01-29	GR01-30	GR01-31	GR01-32	GR01-45	GR01-82	GR01-89	GR01-90	GR01-92	GR01-93	GR01-94	GR01-98	GR00-45
Ag	15.75	70.8	17.2	0.42	0.24	0.58	1.42	0.36	0.22	30.7	34	14.8	199	61.6	28	87.2	35.3	182	52
As	1735	124	1510	1485	1565	1470	72.8	371	604	427	257	9380	158.5	123	179	154.5	149	1615	282
Au	350	1920	730	16	8	28	440	19	2	590	2800	230	8500	1600	1210	5100	3100	1060	1170
Bi	1.9	11.9	19.0	10.7	17.1	61.1	11.3	4.5	0.9	4.9	17.8	3.2	71.0	5.9	3.9	1.8	1.8	71.2	81.7
Cd	0.7	>500	6.06	3.84	0.64	0.42	1.76	0.84	0.8	5.44	1.32	1.2	63.9	9.14	8.1	7.48	3.3	9.1	8.18
Ce	59.5	38.3	80.2	72.4	79	60.7	60.5	21.3	44	32.2	10.85	38.5	21.3	33.2	52.4	39.7	48.9	17.2	19.95
Co	5.5	337	4.6	8.7	3	6.6	8.9	4.6	3.3	2.6	428	7	361	26.6	8.4	28.6	21.3	8	9.2
Cr	153	108	109	139	83	100	130	138	61	157	79	90	144	119	90	115	94	70	140
Cu	7910	40300	9490	99.6	71.4	82.2	803	78	213.8	12200	8790	98.6	71000	21400	13800	46600	16600	58000	33600
F	320	190	170	120	140	100	550	300	100	220	300	400	210	300	200	230	200	380	1350
Fe	15.5	13.15	16.4	18	15.95	17.85	14.25	14.3	16.5	14.9	15.45	6.09	20.2	12.3	12.75	14.15	13.15	18.75	15
Ga	15.65	14.55	17.25	13.75	19	18.9	23.65	13.5	14.55	16.55	2.65	20.5	6.25	9.8	20.2	14.35	18.15	13.5	8.25
Ge	0.05	0.5	0.3	0.15	0.2	0.25	0.35	0.3	0.15	0.4	0.25	<0.50	0.55	1.05	0.9	0.5	1	<0.50	7.85
Hg	90	90	10	10	10	<10	30	10	<10	70	10	100	40	10	20	50	20	140	10
In	5.96	33	8.32	2.83	2.95	3.1	10.45	4.93	3.22	7.13	6.53	1.2	15.7	10.6	10	22	11.4	11.3	9.11
K	<0.01	<0.01	<0.01	0.03	0.02	0.09	3.62	0.16	0.21	<0.01	0.03	0.63	<0.01	<0.01	<0.01	<0.01	<0.01	3.03	0.03
La	29	9	35	33	35.5	28	48	10.5	16.5	13	4.5	25	6	8.5	15.5	11	12.5	10	12.5
Mg	0.09	0.64	0.17	0.08	0.11	0.06	0.6	0.63	0.05	0.08	2.67	1.92	2.25	1.59	0.91	0.56	0.77	0.23	0.35
Mn	1785	1820	1700	1580	1870	1710	315	2770	1625	2280	785	2050	1660	1435	1630	1435	1470	900	1760
Mo	2.85	2.05	19.9	3.3	2.6	4.15	587	84	13.95	29.85	7.5	6	5.45	4.05	4.55	4.15	3.05	2.44	6.95
Na	<0.01	<0.01	<0.01	<0.01	<0.01	<0.01	0.17	<0.01	<0.01	<0.01	<0.01	0.95	<0.01	<0.01	<0.01	<0.01	<0.01	0.18	<0.01
Ni	75.9	509	100.5	17.2	14.6	18.6	32.8	22.4	14.4	123.5	34	20	700	210	156	570	150	32	49.6
P	160	1110	390	70	120	10	1530	1200	<10	340	2270	1900	1560	1470	750	940	730	1600	6660
Pb	4	8	5	22	6	7.5	14	11	8	7.5	7	330	18.5	7.5	8	88.5	12.5	300	207
S	2.45	>10.00	2.15	7.38	1.07	5.88	>10.00	1.77	0.75	1.77	>10.00	0.2	>10.00	2.55	1.44	5.34	1.77	6	3.27
Sb	9.05	7.95	6.45	28.45	5.35	7.85	10.1	11.65	12.9	17.35	18.15	34.35	20.9	13.05	7.25	26	8.3	196.5	225.8
Se	6	79	7	7	<1	8	22	1	<1	2	54	<10	49	5	4	21	7	40	9
Sn	5.6	11	6.2	3.4	3.4	3.4	18.2	14	5.6	8.4	4.4	6	7.4	15	22.6	18.4	18.2	2	8.4
Te	1.5	4.4	3	6.35	0.95	38.2	10.75	3.3	0.9	7.15	0.5	0.5	6.55	2.9	0.15	0.9	0.4	15	35.6
Tl	<0.02	0.8	0.06	0.06	0.04	0.06	1.7	0.12	0.08	0.06	0.16	6.6	0.42	0.22	0.26	2.02	0.34	2.8	0.76
U	19.7	18.3	19	22.4	22.2	18.7	7.2	14.8	13	12.5	2.2	6	10.5	15.8	15.3	12.2	16.8	4	5.3
W	425	209	349	438	404	415	27.4	409	291	206	13.7	5	112	190.5	276	193	269	63	131
Zn	52	214000	642	356	26	<2	10	14	22	416	154	140	8930	920	760	740	286	720	880

**Sample descriptions & locations:**

- GR01-9: LD01-32: 317 feet. Massive brown-green garnet skarn with chalcopyrite. 346939E 6162113N
- GR01-20: LD99-17: 275 feet. Green garnet skarn with sphalerite and chalcopyrite.
- GR01-22: LD20-12: 211 feet. Massive garnet skarn with chalcopyrite. 346965E 6162128N
- GR01-23: LD20-17: 556 feet. Coarse brownish green crystalline garnet skarn with pyrite. 346930E 6162150N
- GR01-24: LD20-17: 572 feet. Massive brown garnet skarn with pyrite. 346930E 6162150N
- GR01-28: LD01-32: 407 feet. Massive dark garnet skarn with pyrite. 346939E 6162113N
- GR01-29: LD01-32: 197 feet. Massive garnet skarn with pyrite. 346939E 6162113N
- GR01-30: LD01-32: 229 feet. Brown garnet with retrograde alteration and pyrite veinlets. 346939E 6162113N
- GR01-31: LD97-11: 289 feet. Brown garnet skarn with sulphides.
- GR01-32: LD 97-11: 494 feet. Greenish garnet skarn with sulphides.
- GR01-45: LD20-07: 332 feet. Retrograde altered garnet-chlorite-pyrite-pyrrothite-chalcopyrite skarn 0.75m from marble.
- GR01-82: Pyrite-epitaxial skarn near dike contact. 346748E 6161809N
- GR01-89: LD20-06: 330 feet. Garnet skarn with pyrite and chalcopyrite.
- GR01-90: LD20-06: 332 feet. Brown garnet skarn with disseminated pyrite and chalcopyrite.
- GR01-92: LD20-09: 267 feet. Brown, green and pink garnet skarn with pyrite and chalcopyrite.
- GR01-93: LD20-09: 271 feet. Pale green garnet skarn (minor brown garnet) with pyrite and chalcopyrite.
- GR01-94: LD20-09: 282 feet. Pale green coarse grained garnet skarn with disseminated pyrite and chalcopyrite.
- GR01-98: Brown and green garnet skarn and massive pyrite-chalcopyrite at drill-pit LD99-04. 347015E 6162122N
- GR00-45: North Canyon Zone. Garnet-chalcopyrite-pyrite skarn. 346991E 6162139N

**TABLE 2C**  
**ASSAY DATA OF SPHALERITE-BEARING MANTO SAMPLES, NUMBER 3 AND 4B ZONES, LUSTDUST PROPERTY**

No.	GR01-43	GR01-78	GR01-79	GR01-80	GR01-99	GR01-100	IWE01-3	GR00-43	GR00-44	GR01-19	GR01-39	GR01-40	GR01-42	GR01-49	GR01-88
Ag	8.8	151	68	36.6	223	13	9.2	10.85	121	20.3	8.62	13.2	64.7	21.8	444
As	235	>10000	>10000	>10000	289	2270	390	651	2420	56	1855	1635	383	627	27.6
Au	16	1430	4700	1200	2500	990	125	91	1190	580	280	340	770	2100	26050
Bi	0.7	193	59.9	87.6	1450	54.3	42	40.1	259	12.9	10.8	9.3	3.9	165.0	44.6
Cd	46.4	230	4.6	210	>500	10.55	>500	>500	>500	>500	>500	>500	257	>500	>500
Ce	1.18	0.9	<0.10	1	1.3	2.6	7.4	7.94	1.39	3.89	2.67	3.48	0.83	6.03	1.52
Co	3.6	<1.0	<1.0	1	<1.0	25	39	19.4	0.8	575	2.3	3.5	17.1	9.6	906
Cr	12	80	20	40	30	160	70	24	103	43	79	93	60	74	12
Cu	168.8	805	247	1320	15000	213	1165	629	330	6510	1025	1680	245	1290	159000
F	90	60	50	60	90	50	80	130	40	120	30	60	380	340	40
Fe	3.99	>25.0	>25.0	>25.0	12.9	>25.0	21.5	12.65	22.8	7.52	>25.0	>25.0	22.1	12.45	>25.0
Ga	0.8	8.5	2.5	5.5	26	1	13	17.9	5.1	2.4	7.9	6.85	1.8	17.15	0.6
Ge	<0.05	0.5	<0.50	0.5	<0.50	<0.50	<0.50	14.35	25.25	0.45	0.7	0.65	0.5	0.45	0.9
Hg	70	3490	510	1240	90	40	470	810	290	190	310	330	170	100	60
In	0.355	31.1	0.55	23.1	13.15	0.3	26.5	29	2.5	27.1	12.65	8.39	3.95	38	26.1
K	<0.01	0.05	<0.01	0.03	<0.01	0.03	0.01	<0.01	<0.01	<0.01	<0.01	<0.01	0.05	0.03	<0.01
La	3	<5.0	<5.0	<5.0	<5.0	<5.0	5	7.5	5	2	3	3	6.5	5	1
Mg	0.19	0.03	0.03	0.01	0.49	<0.01	0.46	0.17	0.01	1.17	0.01	0.03	0.12	0.21	0.14
Mn	840	50	<50	100	3350	50	1600	2060	845	3750	840	845	525	1905	935
Mo	0.45	19	0.5	32.5	2	1	<0.50	1.55	2.6	0.75	2.1	1.35	1	1.1	9.5
Na	<0.01	0.03	0.03	0.03	<0.01	0.03	<0.01	<0.01	<0.01	<0.01	<0.01	<0.01	<0.01	<0.01	<0.01
Ni	19.6	4	6	10	6	8	18	14.6	3.8	93.6	<0.2	<0.2	4.6	8	2460
P	260	1400	<100	1200	<100	<100	200	340	50	590	20	40	30	230	1610
Pb	5010	11600	2820	9830	760	320	120	316	67400	7.5	40.5	34.5	145500	231	11.5
S	4.77	0.4	0.2	0.2	>10.00	>10.00	>10.00	>10.00	>10.00	>10.00	>10.00	>10.00	>10.00	>10.00	>10.00
Sb	>1000.0	>1000.0	>1000.0	>1000.0	164	254.5	107.5	309	>1000.0	4.1	23.25	22.1	>1000.0	152.2	14
Se	2	<10	20	<10	50	50	70	60	113	121	62	57	78	94	190
Sn	0.2	<2.0	<2.0	<2.0	8	<2.0	2	1	3.2	2	1	1	6	1.6	1
Te	0.8	1	12.5	0.5	37	12.5	12.5	4.5	78.4	1.15	4.25	4.75	6	66.4	13.35
Tl	0.06	84.8	56.2	5	1	2.6	0.4	5.24	0.9	0.12	0.04	0.04	0.3	0.12	0.4
U	2.2	16	2	21	2	<1.0	2	1.6	1.6	2.8	2.5	2.4	2.3	4.2	0.5
W	1.6	52	9	30	297	8	20	59.9	0.5	61.2	24.7	36.6	10.2	21.1	5.7
Zn	4500	23000	480	15900	474000	1220	316000	436000	142500	437000	176500	164000	42000	415000	141500

Sample descriptions & locations:

- GR01-43: LD93-11; 32.9 metres. Oxidized mineralization in marble.  
 GR01-78: No. 3 Zone. Light and dark vuggy oxidized material from trench. 347552E 6161102N  
 GR01-79: No. 3 Zone. Light and dark vuggy oxidized material from trench. 347552E 6161102N  
 GR01-80: No. 3 Zone. Light and dark vuggy oxidized material from trench. 347552E 6161102N  
 GR01-99: No. 4B Zone. Massive black sphalerite with coarse pyrite-pyrrhotite. 347096E 6161452N  
 GR01-100: No. 4B Zone. Massive black sphalerite with coarse pyrite-pyrrhotite. 347096E 6161452N  
 IWE01-3: No. 4B Zone. Massive sphalerite with coarse pyrite. 347085E 6161470N  
 GR00-43: 4B Zone. Massive sphalerite-pyrite. 437096E 6161459N  
 GR00-44: No. 4B Zone. Massive sphalerite-pyrite. 437096E 6161459N  
 GR01-19: LD99-17; 266 feet; No. 4B (transition) Zone. Sphalerite and chalcopyrite.  
 GR01-39: LD93-8; 20.4 metres. Massive black sphalerite with pyrite. 347112E 6161510N  
 GR01-40: LD93-8; 21.5 metres. Massive black sphalerite-pyrite with white quartz veining. 347112E 6161510N  
 GR01-42: LD93-8; 31 metres. Massive sphalerite with 20% coarse euhedral pyrite. 347112E 6161510N  
 GR01-49: LD92-15; 32 metres. Massive black sphalerite with pyrite.  
 GR01-88: LD20-06; 329 feet. Massive to semi-massive sphalerite with pyrite and chalcopyrite. 347005E 6161743N

presence of very large decrepitation fluid inclusions (*see* Photo 5, Dunne and Ray, 2002, this volume). Locally, they contain abundant small fibrous inclusions of unknown composition and origin (Leitch, 2001a).

Where the skarns contain sulphide mineralization, the late, pale to dark green and weakly pleochroic chlorite may make up to 10 % of the rock. Mineralization occurs as Ag and Au-bearing chalcopyrite and lesser bornite with abundant pyrite, variable amounts of sphalerite and rare arsenopyrite and stibnite. It is commonly controlled by fractures but may be disseminated. Megaw (2000, 2001) notes that the conduit structures through the garnetite are often surrounded by zones, several metres wide, of more disseminated mineralization. The density of mineralized structures, the width of their disseminated haloes, and the intensity of

retrograde alteration increase with both depth and proximity to the Canyon Creek Fault (Figure 2). Retrograde alteration is often accompanied by a dramatic increase in chalcopyrite, pyrite and magnetite. The latter mineral occurs either as fine-grained masses or as pseudomorphs, up to 2 mm long, after bladed specularite. The chalcopyrite commonly occurs as interstitial blebs and masses up to 6 mm in length. However, chalcopyrite is also seen as small (<0.5 mm), rounded to irregular inclusions in sphalerite and magnetite (Leitch, 2001a). Also present are variable quantities of specular hematite, marcasite and relict pyrrhotite. In rare cases, the skarn may contain up to 30 % sphalerite (Table 2B), as well as trace amounts of a fibrous, dark grey mineral that may be tetrahedrite-tennantite. The dark, red-brown subhedral sphalerite crystals reach 2 mm in length.

**TABLE 2D**  
**ASSAY DATA OF MASSIVE PYRITE-PYRRHOTITE REPLACEMENTS, 4B ZONE, LUSTDUST**

No.	GR01-21	GR01-41	GR01-44	GR01-46	GR01-47	GR01-48	GR01-67
Ag	54.7	20	5.14	3.24	5	3.04	15.45
As	428	3530	792	1710	>10000	>10000	324
Au	1840	110	400	84	680	550	960
Bi	1165.0	48.5	18.9	14.1	27.6	9.2	74.6
Cd	15.5	>500	4.08	4.8	2.98	1.66	1.76
Ce	1.2	25.8	1.12	7.74	2.37	25.3	12.15
Co	178.2	8	15.4	36.1	21.3	55.2	17.1
Cr	58	59	48	183	103	105	73
Cu	15600	864	891	556	828	405	4750
F	100	2500	320	670	300	210	520
Fe	>25.0	>25.0	>25.0	>25.0	>25.0	24.5	>25.0
Ga	1.1	5.9	1.45	2.85	1.25	7.95	8.45
Ge	0.85	0.9	0.65	0.5	0.75	0.65	1.65
Hg	<10	390	<10	10	30	10	<10
In	3.19	3.95	0.07	0.09	0.07	0.075	3.98
K	<0.01	0.51	0.07	0.03	0.04	0.4	<0.01
La	0.5	28	1	6	2	12.5	9.5
Mg	0.29	0.88	0.38	0.28	0.1	0.69	0.29
Mn	725	910	200	375	385	575	545
Mo	1.2	42.35	0.75	1.65	1.4	5.3	3.8
Na	<0.01	<0.01	<0.01	<0.01	<0.01	<0.01	<0.01
Ni	2.8	22.8	7	17.2	14.8	33.8	31.4
P	380	1110	<10	4060	1420	330	2990
Pb	43.5	27800	325	2360	335	205	29
S	>10.00	>10.00	>10.00	>10.00	>10.00	>10.00	>10.00
Sb	31.05	>1000.0	247.7	>1000.0	434	453.9	15.5
Se	95	29	36	13	5	2	39
Sn	2.4	1.6	0.4	0.2	<0.2	1.2	12
Te	129	6.45	12.3	2.1	0.55	1.4	63.2
Tl	0.02	1.22	0.22	0.1	0.08	0.52	0.12
U	3.4	14.5	4	0.5	0.1	1.2	10.7
W	23.3	15.3	2.3	4.1	12.8	74.9	18.5
Zn	1655	122500	354	410	220	136	164

Sample descriptions & locations:

GR01-21: LD99-17; 192 feet. 4B zone; 1.2 metre wide massive pyrite-pyrrhotite-chalcopyrite in marble.

GR01-41: LD93-8; 27.2 metres. Massive pyrrhotite with sulphosalts. 347112E 6161510N

GR01-44: LD93-11; 46 metres, 1 metre wide zone of massive pyrrhotite in bleached marble.

GR01-46: LD93-4; 88 metres. Massive pyrite-pyrrhotite with sulphosalts.

GR01-47: LD93-4; 90 metres. Massive pyrite-pyrrhotite with white quartz blebs. 347153E 6161265N

GR01-48: LD93-4; 91.5 metre. Massive pyrrhotite-pyrite and white quartz blebs. 347153E 6161265N

GR01-67: LD20-07; 295 feet. Massive pyrite-pyrrhotite-chalcopyrite zone 1 metre from hornfels contact (at 301 feet).

Cross-cutting relationships show that the bulk of the Canyon Creek skarn formed early during an evolving, cyclic process that generated enormous volumes of garnet ± pyroxene assemblages. These features suggest the presence of a potent, long-lived hydrothermal system that resulted in skarn replacement of the limestone, intrusions and previously hornfelsed argillite. The subsequent mineralization was controlled by structures, crystal grain boundaries, and other geologic discontinuities or lithological contacts in the skarn.

The skarn's outer contact with the country rocks is commonly sharp, the very pale brown-green garnet passing out to a narrow (< 2 metres) zone of strongly bleached marble. Locally, the marble-skarn contacts are occupied by ir-

regular blebs and narrow zones of massive sulphide mineralization containing sphalerite, pyrite, pyrrhotite and minor chalcopyrite. Megaw (1999) considers these to be a transitional style of mineralization between the skarns and the more distal mantos.

### ***MANTOS (NUMBERS 2, 3 AND 4B ZONES)***

The Canyon Creek skarn passes southwards into a number of more or less stratigraphically concordant massive sulphide mantos and their oxidized equivalents. The mantos are best developed along permeable carbonates, particularly where these rocks are in close proximity to chlorite-altered mafic tuff beds. They tend to occur as

**TABLE 2E**  
**ASSAY DATA OF SULPHIDE AND**  
**SULPHOSALT-BEARING VEINS, NUMBER 1 ZONE**  
**(TAKLA SILVER MINE), LUSTDUST PROPERTY**

No.	GR01-5	GR01-26	GR01-27	GR01-101	GR01-42
Ag	167	6277.2	5513.4	1030	840
As	>10000	>10000	>10000	>10000	>10000
Au	4300	6400	4200	12050	4800
Bi	1.1	0.5	0.6	3.5	1.21
Cd	246	301	176	81.6	52.7
Ce	0.9	0.4	<0.10	0.2	0.64
Co	<1.0	<1.0	<1.0	<1.0	0.4
Cr	140	60	80	40	117
Cu	198.3	7980	4110	1000	861
F	40	30	30	30	40
Fe	19.4	7.18	5.34	14.65	9.6
Ga	3	5	2	0.5	1.5
Ge	0.5	<0.50	<0.50	<0.50	7.9
Hg	16510	>100000	62500	11560	19150
In	1.9	0.25	0.25	0.15	0.15
K	0.04	0.01	0.01	<0.01	<0.01
La	5	10	10	10	4
Mg	<0.01	<0.01	0.01	<0.01	<0.01
Mn	50	350	550	300	290
Mo	<0.50	<0.50	<0.50	6	5.1
Na	0.03	0.02	0.02	0.03	<0.01
Ni	2	8	<2.0	4	3.8
P	<100	<100	<100	<100	120
Pb	68300	146000	223000	158000	57300
S	>10.00	>10.00	>10.00	>10.00	8.78
Sb	>1000.0	>1000.0	>1000.0	>1000.0	>1000.0
Se	<10	<10	<10	<10	<1
Sn	6	16	30	16	5.6
Te	<0.50	<0.50	<0.50	0.5	0.05
Tl	>500	>500	>500	310	>500
U	1	2	2	3	0.8
V	<10	<10	<10	<10	3
W	1	<1.0	<1.0	2	0.4
Zn	2920	31900	11000	820	2230

Sample descriptions & locations:

GR01-5: Pyrite, sulphosalts, arsenopyrite, scorodite.

347853E 6160749N

GR01-26: No. 1 Zone. Pyrite, sulphosalts, arsenopyrite, scorodite.

347855E 6160516N

GR01-27: No.1 Zone. Pyrite, sulphosalts, arsenopyrite, scorodite with

white quartz. 347860E 6160518N

GR01-101: No.1 Zone. White quartz vein with tetrahedrite-pyrite.

347860E 6160518N

GR00-42: No. 1 Zone. Sphalerite-sulphosalts. 349647E 6159929N

flat-lying to gently-inclined, elongate zones developed along structurally thickened and deformed antiformal crests. However, drilling has not revealed any substantial chimney feeders for these bodies, which appear to be stacked in successive limestone beds, resulting in “saddle-reef” morphologies (Megaw, 1999). From south to north the clusters of mantos have been designated the Numbers 2, 3 and 4B-Zones (Figure 2; Evans, 1996, 1997; Megaw, 2001). They crop out in an en echelon fashion (Figure 2), and the northernmost bodies, the Number 4B Zone, appear to merge into the Canyon Creek skarn.

The 4B Zone is well exposed in a number of trenches and its mantos and carbonate replacements appear to be developed along a tight, gently northwest plunging antiformal fold whose axial plane is steeply west dipping. The aligned

**TABLE 3**  
**AVERAGE ASSAY VALUES AND METAL RATIOS FOR**  
**THE VARIOUS STYLES OF MINERALIZATION,**  
**LUSTDUST PROPERTY**

	Glover Stock Porphyry	Canyon Creek Skarn	No. 4B Zone		No. 1 Zone Distal veins
			Pyrrhotite & pyrite-rich masses (n = 7)	Sphalerite- rich mantos (n = 15)	
Hg (ppb)	6	38	65	545	41944
Au ppb	5	1520	661	2824	8150
Ag	0.4	43.8	15.2	81	2765.5
As	39	1140	3826	2723	>10000
Ba	1326	59	26	106	77
Bi	0.5	21	194	162	1.4
Cd	4	33	76	351	171
Ce	84.8	43.7	10.8	2.8	0.4
Co	5.4	68	47	107	0.5
Cr	107	112	90	60	87
Cs	2.1	0.9	0.8	0.3	4.5
Cu	106	17955	3413	12642	2830
F	708	304	660	108	34
Ga	18.2	14.8	4.1	7.8	2.4
Ge	0.2	0.8	0.9	3.0	1.8
Hf	2.82	4.86	0.31	3.66	2.80
In	0.1	9.0	1.6	16.2	0.5
La	50.2	19.1	8.5	3.6	7.8
Li	3.5	1.8	7.5	1.1	7.8
Mn	216	1609	531	1181	308
Mo	467	54	8	5	2
Ni	7	150	19	177	4
P	1118	1201	1471	408	64
Pb	31	56	4443	16267	130520
Rb	81.4	17.0	15.1	1.9	1.6
Nb	13.3	2.3	0.9	0.6	1.5
Sb	23	51	455	470	1000
Se	1.6	17.2	31.3	65.1	4.1
Sn	0.8	9.6	2.6	2.1	14.7
Sr	763	23	9	26	9
Te	0.3	7.3	30.7	17.0	0.3
Th	29.9	20.4	0.9	25.9	39.6
Tl	0.9	0.9	0.3	10.5	462
U	4.0	13.5	4.9	4.2	1.8
W	4	233	22	43	1
Zn	368	12056	17920	185673	9774
Al (%)	6.76	1.29	0.46	0.06	0.02
Ca (%)	1.82	13.51	0.85	2.56	0.08
Fe (%)	1.75	14.98	24.93	19.39	11.23
K (%)	2.57	0.42	0.15	0.02	0.02
Mg (%)	0.69	0.72	0.42	0.21	0.01
Na (%)	2.38	0.08	0.01	0.02	0.02
S (%)	0.60	4.41	>10	7.70	9.76
Cu/Au	22848	18043	4583	4123	506
Cu/Ag	296	415	183	88	1
Zn/Pb	16	1460	7	5740	0.1
Zn/Au	63522	8162	160149	670805	1763
Ag/Au	94	41	42	88	519
Cu/Mo	4.50	3563	2352	2828	9898

massive sulphide pods follow either the fold crest or a thrust that separates limestones from hornfelsed graphitic phyllites further east (Megaw, 2001). A mafic tuff horizon within the limestone appears to have been an important conduit for fluid movement. There are two styles of mineralization in the 4B Zone. The most common and economically important comprises 10 to 50 % massive, dark brown to black sphalerite with variable amounts of pyrite ± arsenopyrite ± well-zoned pyrrhotite ± chalcopyrite ± an unidentified grey, fibrous sulphosalt mineral that may be boulangerite, bournonite and/or tetrahedrite-tennantite (Leitch, 2001b). Calc silicate minerals generally make up < 1% of the rock and may include thin veins of chloritized clinopyroxene.

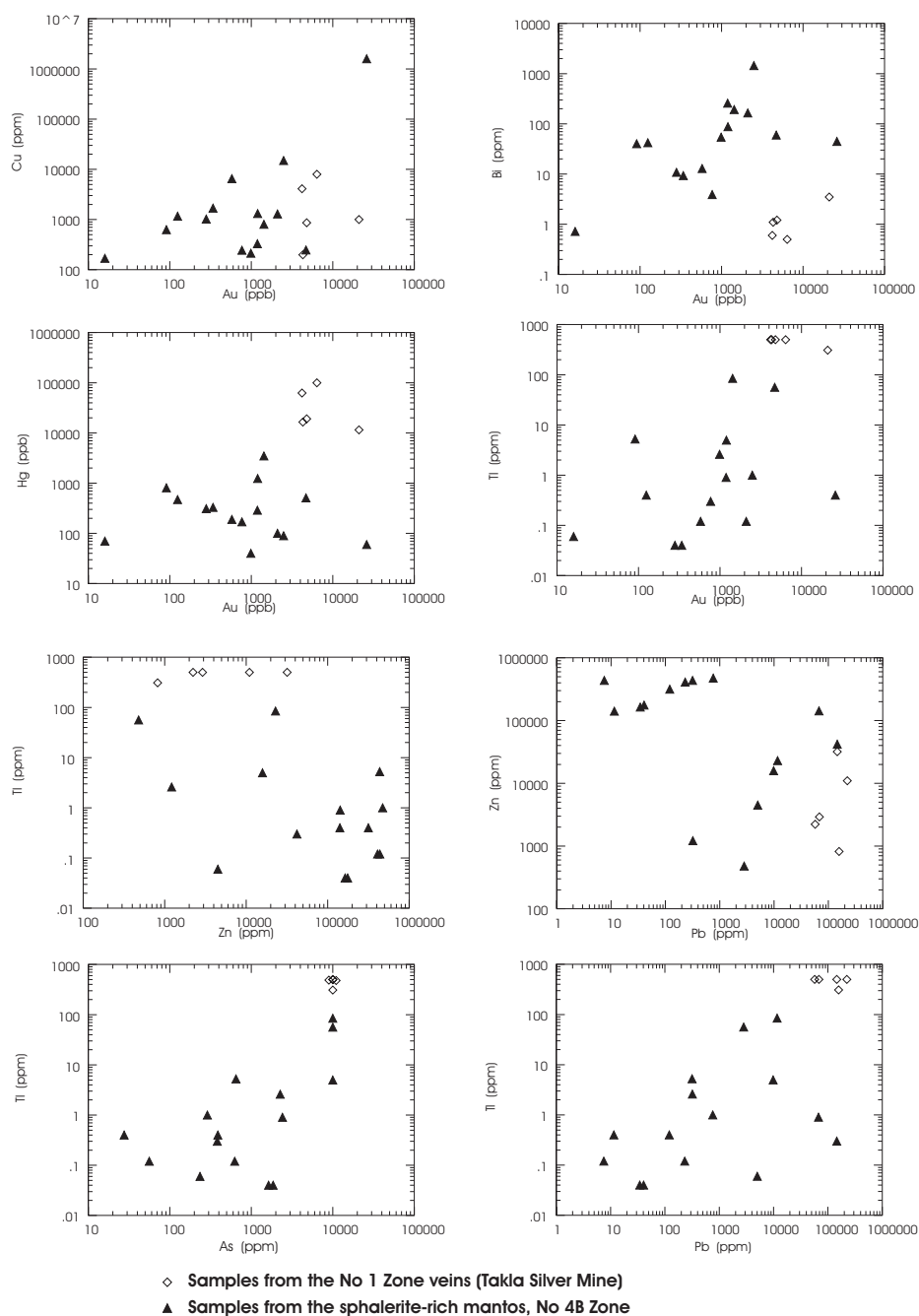


Figure 6. Plots comparing the chemistry of the Number 1 Zone veins (open diamonds) and the sphalerite-rich mantos (filled triangles), Lustdust property. Data from Tables 2C and 2E.

The other style occurs as small (commonly < 1.5 m thick) pods and veins of coarse-grained pyrite-pyrrhotite-dominant mineralization. Pyrite both replaces, and is replaced by, pyrrhotite. Sphalerite in this style of mineralization is generally less abundant (< 10 %), although arsenopyrite, sulphosalt minerals and trace amounts of galena are sporadically developed (Table 2D).

Polished thin section studies (Leitch, 2001a) indicate the subhedral to euhedral sphalerite crystals in the 4B Zone to be almost opaque, suggesting a high Fe content. The crystals

reach 3 mm in diameter and contain small (< 25 microns) inclusions of pyrrhotite and larger inclusions of an unidentified bladed silicate. Pyrrhotite and/or pyrite may each locally exceed 50 % of the mineralization. The former mineral comprises subhedral lath-shaped crystals up to 0.5 mm long whereas pyrite cubes, up to 0.75 cm, contain irregular core zones with abundant small silicate inclusions. Gangue minerals include up to 5 % sericite with lesser secondary quartz, calcite and amorphous limonite.

Contacts between the massive sulphides in the 4B Zone mantos and the bleached, recrystallized limestone country rocks are generally very sharp. Replacement features include “scaloped” contacts and in some bodies the massive sulphides contain small, (< 0.3 m) round and isolated remnants of altered limestone. Drilling parts of the 4B Zone between 1992 and 1999 indicates a probable resource of 250,000 tonnes grading 1.3 g/t Au, 12 g/t Ag and 5.5 % Zn with possible Pb, Cu, In, Ge and Ga credits (Megaw, 2001).

The 3-Zone further south (Figure 2) contains the largest manto resource identified at Lustdust. It is entirely oxidized to a 50 m depth, possibly due to pre-glacial weathering. Below this depth, drilling intersects primary pyrite, pyrrhotite and sphalerite with elevated Au grades (Megaw, 2000, 2001). The thickest portions of the 3 Zone mantos occupy the crest of a small-scale anticline and are hosted by carbonates that are interbedded with mafic tuffs. Surface trenching reveals local sections assaying up to 17.9 g/t Au and 69.4 g/t Ag over 4 metres. Drilling from the 1950's to 1991, outlined a probable oxide resource of 650,000 tonnes grading approximately 3 g/t Au, 20 g/t Ag and 5 % Zn (Megaw, 2001).

The Number 2 Zone represents the most southerly development of manto mineralization at Lustdust (Figure 2). It is a minor oxidized replacement zone similar to the 3-Zone further north. However, it is probably controlled by a small synform and mineralization is traceable for 200 m along strike. Surface sampling (Megaw, 2001) indicates an average of 2.3 g/t Au, 109 g/t Ag, 2.16 % Zn and 2.09 % Pb across 5.3 meters true width.

### **NUMBER 1 ZONE VEINS**

The Number 1 Zone veins at the southern end of the property were the target for exploration in the 1940's that led to the underground test workings at the former Takla Silver Mine (Figure 2). In this vicinity, bleached and recrystallized limestones and graphitic phyllites are intruded by numerous thin felsic dikes. At least four, steeply dipping, en echelon, fault-controlled veins and tabular replacements are hosted by the recrystallized limestones or follow dike margins. The veins comprise largely sulphides and sulphosalts with some open-space filling by quartz and calcite. In some outcrops the vein quartz is brecciated and recemented by later quartz and/or calcite. The principal quartz-sulphide vein was explored by underground drifting and drilling in the 1940's and 1960's. Sutherland Brown (1965) and Mathieu and Bruce (1970) identified a number of sulphide, arsenides, and complex sulphosalt minerals, including sphalerite, pyrite, stibnite, boulangerite (Pb<sub>5</sub>Sb<sub>4</sub>S<sub>11</sub>) and realgar. Mathieu and Bruce (1970) noted differences in the mineralogies of the underground and surface trench samples. The latter were oxidized and included a variety of Pb antimonides and secondary Pb-bearing minerals, such as jamesonite, zinkenite, anglesite and Tl-bearing twinnite. In addition, the surface samples contained sphalerite and Ag-bearing tetrahedrite, tennantite and andorite, as well as valentinite, pyrite, arsenopyrite, covellite, chalcopyrite, and scorodite Fe(AsO<sub>4</sub>) · 2H<sub>2</sub>O with a gangue of quartz and dolomite. The underground samples had fewer Pb antimonides; the major ore minerals identified included ar-

senopyrite, pyrite, with lesser sphalerite and jamesonite (Pb<sub>4</sub>FeSb<sub>6</sub>S<sub>14</sub>) and minor amounts of andorite, argentiferous tetrahedrite, miargyrite, realgar, stibnite and chalcopyrite in a gangue of quartz, calcite and minor dolomite. No gold was observed in the mineralogical study (Mathieu and Bruce, 1970), but their tests suggested the metal was associated with pyrite and arsenopyrite.

In a polished thin section study, Leitch (2001a) tentatively identified the presence of bournonite (PbCuSbS<sub>3</sub> (2PbS.Cu<sub>2</sub>S.Sb<sub>2</sub>S<sub>3</sub>)). The abundant quartz consists of zoned crystals up to 4 mm across, and the arsenopyrite is distinctly more fractured than the pyrite. The sphalerite crystals, which are intergrown with secondary quartz and arsenopyrite, are strongly zoned with dark cores and paler rims.

### **CHEMISTRY OF THE LUSTDUST MINERALIZATION**

For this study, mineralized samples were collected from the Glover Stock porphyry, the Canyon Creek skarn, the sphalerite-rich and pyrite-pyrrhotite replacements in the 3 and 4B zone mantos, and the distal Number 1 Zone veins. The analytical data for these five styles of Lustdust mineralization are presented in Tables 2A to 2E, and the average values and metal ratios are summarized in Table 3. These data demonstrate the north to south chemical zoning at Lustdust. The porphyry has the highest Mo content (average 467 ppm) and there is a progressive decrease in this metal in the skarn, mantos and more distal veins (Table 3). The highest Cu values occur in the Canyon Creek skarn and the 4B sphalerite-rich mantos (averages 17955 ppm and 12642 ppm respectively), while the Number 1 Zone veins and the porphyry have a much lower Cu content.

Unlike Cu and Mo, virtually all the other metals and pathfinder elements listed in Table 3 increase in value towards the more distal, southernmost parts of the mineralized system. The highest average values for Au, As, Hg, Pb, Sb, Sn and Tl are found in the Number 1 Zone veins (Table 3). Exceptions to this include the elements Bi, Cd, Co, Fe, Ni, Se, Te and Zn which occur in far greater abundances in the two styles of mineralization present in the 3 and 4B zone mantos (Table 3).

Figure 6 illustrates some of the chemical differences between the Number 1 Zone veins and the 4B Zone sphalerite-rich mantos. The veins generally contain significantly more Hg, As, Au and Tl than the mantos, and in the latter there is a moderate to good positive correlation between Au:Cu. The Zn versus Pb plot in Figure 6 shows the manto samples are separable into low-Pb and high-Pb populations. The high-Pb population is more chemically similar to the Number 1 Zone veins.

Plots of assay data for the Canyon Creek skarn are shown in Figure 7. These demonstrate good positive correlations between Au:Cu, Au:Ag and Ag:Cu. There is also an excellent positive relationship between Bi:Te, suggesting the presence of trace amounts of bismuth tellurides in the skarn. However, no significant correlations are seen between Au:Te, Au:Bi or Au:Fe, and the Au:As plot indicates a weak negative relationship. Figure 7 strongly suggests that

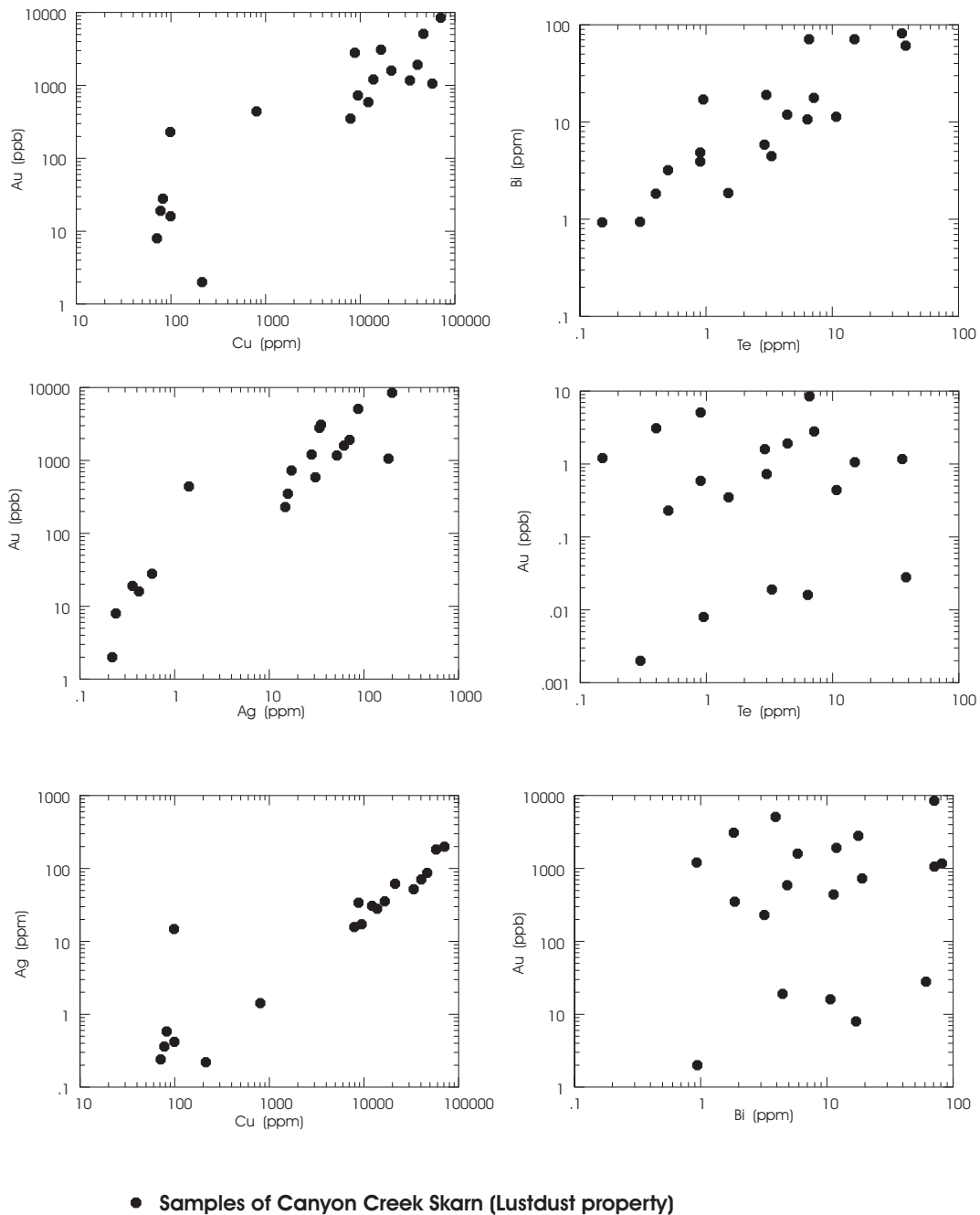


Figure 7. Chemical plots of samples from the Canyon Creek skarn, Lustdust property. Data from Table 2B.

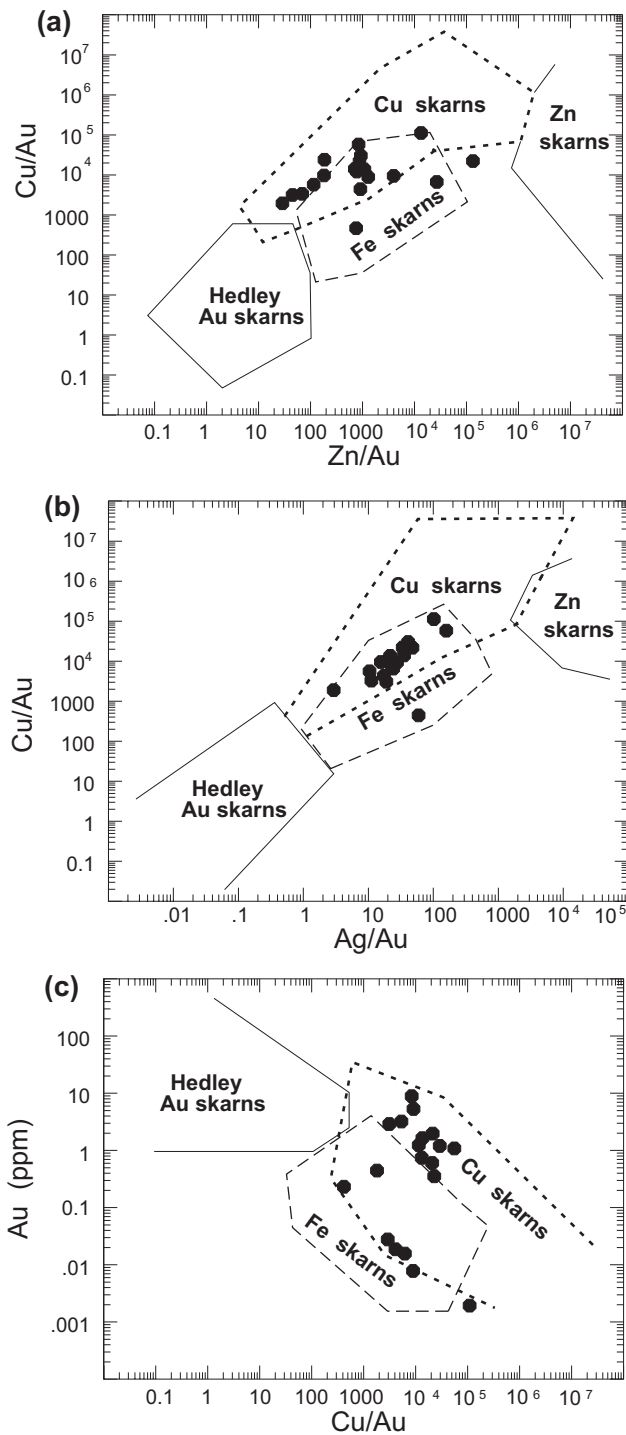
both the Au and Ag in the skarn are associated with chalcopyrite and possibly bornite, and that Au lacks any close association with arsenopyrite or bismuth tellurides. These features, and its Cu: Au, Cu: Ag, Zn: Au and Ag: Au ratios (Table 3; Figure 8) typify Cu skarns rather than the Hedley-type Au skarns (Ray *et al.*, 1996; Ray and Webster, 1997).

## SUMMARY AND CONCLUSIONS

- Alpha Gold Corporation's Lustdust property, which lies 210 km northwest of Prince George, represents one of the

best examples of a zoned porphyry-skarn-manto-vein mineralized system in the Canadian Cordillera.

- Mineralization is developed over a 2.5 km strike length and is related to a small, post-tectonic intrusion, the Glover Stock, and an associated swarm of felsic dikes and sills. The multiphase, composite stock includes mafic dioritic and more leucocratic monzonitic phases, and preliminary U-Pb zircon dates of circa 51-52 Ma on both phases suggest an Eocene intrusive age.
- The stock lies < 2 km west of the Pinchi Fault and it intrudes a deformed package of Cache Creek Terrane argillites, tuffs, cherts and mid to Late Permian lime-



● **Canyon Creek Skarn  
(Lustdust property)**

Figure 8. Metal ratio plots for Canyon Creek skarn samples.

- (a) Cu/Au versus Zn/Au
- (b) Cu/Au versus Ag/Au
- (c) Au versus Au/Cu.

Note the Canyon Creek samples plot within the Cu skarn field. Fields for Au, Cu, Fe and Zn skarns in BC from Ray *et al.* (1996); Ray and Webster (1997).

stones. The north-trending Pinchi Fault separates the Cache Creek rocks from the large, multi-phase Jura-Cretaceous Hogem Batholith in the Quesnel Terrane further east.

- The Glover Stock hosts some Mo porphyry mineralization marked by several generations of barren and sulphide-bearing quartz ± sericite ± K feldspar ± tourmaline veins. Mineralization includes molybdenite with lesser chalcopyrite and rare bornite. This is associated with extensive potassic alteration (K feldspar, sericite and biotite) as well as lesser amounts of albitic metasomatism.
- Outboard from the Glover Stock is developed a north-trending, 2.5 km-long discontinuous belt of mineralization. This comprises the proximal Cu-Au (Zn) Canyon Creek skarn, intermediate Zn (Au, Cu, Pb, Bi) mantos (the 2, 3 and 4B zones) and more distal, sulphide and sulphosalt quartz veins enriched in Au, Ag, Pb, Zn, As, Hg and Tl (the Number 1 Zone).
- Controls of the skarn, manto and vein mineralization include the presence of: (1) permeable carbonates, (2) lithological contacts, including sill-dike margins and limestone-tuff contacts, (3) gently north-plunging fold axes, and, (4) faults and shears.
- The lack of ductile structures within the intrusion, the extensive skarn envelope and the brittle-fracture-control of the veins and some mantos are evidence that the Glover Stock was emplaced at a higher structural level. This conclusion is supported by fluid inclusion studies indicating the system formed at depths between 1.1 km and 1.9 km, assuming a lithostatic regime (Dunne and Ray, 2002, this volume). The much higher depth estimates calculated assuming hydrostatic conditions (Dunne and Ray, 2002, this volume) may reflect episodic over-pressuring followed by structural release to produce the hydrothermal breccias seen in the porphyry, skarn and Number 1 Zone veins.
- The Eocene age of the Glover Stock and its REE chemistry (Figure 5) are strong evidence that the stock and the mineralization are not related to the nearby Jura-Cretaceous Hogem Batholith (Figure 1). Instead, the stock may belong to a widespread suite of Eocene plutons, some of which are associated with Cu mineralization. One example includes the intrusions in the Babine porphyry Cu belt (Dirom, 1995; Schiarizza and MacIntyre, 1999), situated approximately 80 km southwest of Lustdust. Another possible body of this type intrudes Cache Creek Terrane rocks at Rubyrock Creek, approximately 100 km south of Lustdust (MacIntyre and Schiarizza, 1999).
- Gold-bearing Cu skarns and Zn mantos associated with Mo porphyry systems are rare and there are few reported analogues to the Lustdust property in British Columbia. Foreign examples may include the Antamina and Magistral porphyry-skarn deposits in Peru (Redwood, 1999; Northern Miner, 2001). These deposits differ in a number of ways from Lustdust, including their geological setting (continental shelf-carbonates versus oceanic carbonates). However, similarities include (1) a large and metal-rich hydrothermal system related to a shallow-level, Mo-bearing, monzonitic pluton, and (2) an extensive skarn envelope comprising abundant distal green garnet and proximal darker brown garnet. Mineralization at Antamina, like Lustdust, is also Zn-rich.
- The presence at Lustdust of high-grade polymetallic mineralization over a 2.5 km distance suggests a powerful,

metal-rich hydrothermal system. The potential for further discoveries of mineralized mantos, skarn and porphyry on the property is excellent because drilling to depth reveals an increased development of retrograde alteration, sulphides and darker-coloured, proximal-type garnet. Drill intersections through skarn during the 2001 season included hole DDH01-44 which cut 59 m grading 0.8 % Cu and 0.67 g/t Au and hole DDH01-47 which cut 37 m assaying 0.92% Cu and 0.68 g/t Au (Alpha Gold Corp. News release, October 1st 2001).

- The Number 1 Zone veins most likely represent distal mineralization related to the Glover Stock. Alternatively, they could be high sulphidation veins that formed above another buried intrusion related to the Glover Stock (see Figure 9, Dunne and Ray, 2002, this volume). Either of these possibilities, together with the high Hg content of the Number 1 veins, raises exciting chances that some of the numerous Hg occurrences along the Pinchi Fault (Figure 3) represent distal or upper level expressions of hidden, Eocene-age porphyry systems. Thus, the long belt of Cache Creek carbonates along the Pinchi structure warrant exploration for Lustdust-type porphyry-skarn-manto-vein targets (Figure 3), as well as for the other types of mineral deposits suggested by Nesbitt and Muehlenbachs (1988) and Albino (1988).

## ACKNOWLEDGEMENTS

We are grateful to George Whatley, President of Alpha Gold Corp., and his staff for their assistance and hospitality during this project, and for their permission to publish this data. We thank the following: M.J. Orchard (Geological Survey of Canada) for identifying conodont microfossils; R. Friedman (The University of British Columbia) for expediting the preliminary U-Pb zircon dating; C.H.B. Leitch (Vancouver Petrographics Ltd.,) for discussions regarding the ore and plutonic petrography. Editing by Dave Lefebure and Brian Grant is also appreciated.

We dedicate this paper to the memory of our colleague, Keith Glover, who died tragically during this project. The Glover Stock is named for him, as his geological contribution to understanding the deformational history of the area and the structural controls of the mineralization were just beginning to bear fruit.

## REFERENCES

Albino, G.V. (1988): The Pinchi Mercury Belt, central British Columbia: near-surface expression of a Mother Lode-type mineralized system; *Geological Society of America*, Abstracts with Programs, 19:7, A141-142.

Barrie, C.T. (1993): Petrochemistry of shoshonitic rocks associated with porphyry copper-gold deposits of central Quesnellia, British Columbia, Canada; in *Journal of Geochemical Exploration*, 48, Elsevier Science Publishers, Amsterdam, pages 225-258.

Bishop, S.T., Heah, T.S., Stanley, C.R., and Lang, J.R. (1995): Alkalic intrusion hosted copper-gold mineralization at the Lorraine deposit, north-central British Columbia; in *Porphyry Deposits of the Northwest Cordillera of North America*, Schroeter, T.G., Editor, *Canadian Institute of Mining, Metallurgy and Petroleum*, Special volume 46, pages 623-629.

Campbell, D.D. (1966): Summary Geological Report Takla Silver Mines Ltd. Manson Creek, B.C.; Unpublished report by Dolmage Campbell & Associates for *Takla Silver Mines Ltd.*, 17 pages.

Debon, F., and Le Fort, P. (1983): A chemical-mineralogical classification of common plutonic rocks and associations; *Royal Society of Edinburgh*, Transactions, Earth Sciences 73 (for 1982), pages 135-149.

Dirom, G.E., Dittrick, M.P., McArthur, D.R., Ogryzlo, P.L., Pardoe, A.J. and Stohart, P.G. (1995): Bell and Granisle porphyry copper-gold mines, Babine region, west-central British Columbia; In *Porphyry Deposits of the northwestern cordillera of North America*, Schroeter, T.G., Editor, *Canadian Institute of Mining, Metallurgy and Petroleum*, Special Volume 46, pages 256-289.

Dunne, K.P.E., and Ray, G.E. (2002, this volume): Constraints on fluid evolution at the polymetallic Lustdust porphyry-skarn-manto-vein prospect, north-central British Columbia; in *Geological Fieldwork 2001, British Columbia Ministry of Energy and Mines*, Paper 2002-1.

Evans, G. (1996): Geological and geochemical report on the 1996 exploration of the Lustdust property; *British Columbia Ministry of Energy and Mines*, Assessment Report 24735, 125 pages.

Evans, G. (1997): Diamond drilling and geochemical report on the 1997 exploration of the Lustdust property, unpublished report for *Teck Corporation*, 18 pages.

Evans, G. (1998): Diamond drilling report on the 1998 exploration of the Lustdust property; *British Columbia Ministry of Energy and Mines*, Assessment Report 25739, 77 pages.

Gabrielse, H., and Yorath, C.J., Editors (1992): Geology of the Cordilleran Orogeny in Canada. *Geological Society of America*, DNAG G-2, 875 pages.

Garnett, J.A. (1978): Geology and mineral occurrences of the southern Hogen Batholith; *British Columbia Ministry of Mines and Petroleum Resources*, Bulletin 70, 75 pages.

Irvine, T.N., and Baragar, W.R.A. (1971): A guide to the chemical classification of the common volcanic rocks; *Canadian Journal of Earth Sciences*, Volume 8, pages 523-547.

Johnson, D. (1993): Report on trench, diamond drilling and geophysical surveying on the Lustdust property. Unpublished report for *Alpha Gold Corporation*, 11 pages.

Leitch, C.H.B. (2001a): Petrographic report on polished thin sections of 7 samples; *British Columbia Ministry of Energy and Mines*, internal report, 17 pages.

Leitch, C.H.B. (2001b): Petrographic report on 7 thin sections; *British Columbia Ministry of Energy and Mines*, internal report, 8 pages.

Le Maitre, R.W., Bateman, P., Dudek, A., Keller, J., Lameyre, J., Lebas, M.J., Sabine, P.A., Schmid, R., Sorensen, H., Streckeisen, A., Woolley, A.R., and Zanettin, B., Editors (1989): A classification of igneous rocks and glossary of terms: recommendations of the International Union of Geological Sciences Subcommittee on the systematics of igneous rocks, *Oxford Blackwell Scientific Publications*, 193 pages.

MacIntyre, D.G. and Schiarizza, P. (1999): Bedrock geology of the Cunningham Lake map area (93K/ 11, 12, 13, 14), Central British Columbia; *British Columbia Ministry of Energy and Mines*, Open File Map 1999-11, 1:100 000 scale.

Maniar, P.D., and Piccoli, P.M. (1989): Tectonic discrimination of granitoids: *Geological Society of America*, Bulletin, Volume 101, pages 635-643.

Mathieu, G.I., and Bruce, R.W. (1970): Treatment of surface and underground samples of the gold-silver-lead-antimony-zinc ore, from the Omineca Mining District property of Anchor-Takla Mines Ltd., British Columbia; *Department of*

- Energy, Mines and Resources*, Ottawa, unpublished report, 21 pages.
- Megaw, P.K.M. (1999): Report on 1999 drilling and geological study of the Lustdust property, Omineca Mining Division, British Columbia; *British Columbia Ministry of Energy and Mines*, Assessment Report 26069, 151 pages.
- Megaw, P.K.M. (2000): Report on 2000 drilling and geological study of Lustdust property, Omineca Mining Division, British Columbia; *British Columbia Ministry of Energy and Mines*, Assessment Report 26466, 396 pages.
- Megaw, P.K.M. (2001): Report on 2001 drilling and geological study of Lustdust property, Omineca Mining Division, British Columbia; unpublished report for *Alpha Gold Corporation*, 132 pages.
- Meinert, L.D., (1995): Compositional variation of igneous rocks associated with skarn deposits - chemical evidence for a genetic connection between petrogenesis and mineralization; in *Magma, fluids, and ore deposits*, Thompson, J.F.H., Editor, *Mineralogical Association of Canada*, Short Course Volume 23, pages 401-418.
- Monger, J.W.H. (1977): Upper Paleozoic rocks of the western Canadian Cordillera and their bearing on cordillera evolution; *Canadian Journal of Earth Science*, Volume 14, pages 1832-1859.
- Monger, J.W.H. (1998): Plate tectonics and northern cordilleran geology: an unfinished revolution; *Geoscience Canada*, Volume 24:4, pages 189-198.
- Nesbitt, B.E., and Muehlenbachs, K. (1988): Genetic implications of the association of mesothermal gold deposits with major strike-slip fault systems; in *North American conference on tectonic control of ore deposits and the vertical and horizontal extent of ore systems*; *University of Missouri-Rolla*, Proceedings Volume, pages 57-66.
- Northern Miner (2001): Inca Pacific pushed Magistral to prefeasibility. *Northern Miner*, September 24-30, 2001, page 16.
- Paterson, I.A. (1974): Geology of Cache Creek Group and Mesozoic rocks at the northern end of the Stuart Lake Belt, central British Columbia; *Geological Survey of Canada*, Report of Activities, Paper 74-1, Part B, pages 31-42.
- Paterson, I.A. (1977): The geology and evolution of the Pinchi Fault Zone at Pinchi Lake, central British Columbia; *Canadian Journal of Earth Science*, Volume 14, pages 1324-1342.
- Paterson, I.A., and Harakal, J.E. (1974): Potassium-argon dating of blueschists from Pinchi Lake, central British Columbia; *Canadian Journal of Earth Science*, Volume 11, pages 1007-1011.
- Pearce, J.A., Harris, N.B.W. and Tindle, A.G. (1984): Trace element discrimination diagrams for the tectonic interpretation of granitic rocks; *Journal of Petrology*, Volume 25, pages 956-983.
- Ray, G.E. and Webster, I.C.L. (1997): Skarns in British Columbia; *British Columbia Ministry of Employment and Investment*, Bulletin 101, 260 pages.
- Ray, G.E., Dawson, G.L., and Webster, I.C.L., (1996): The stratigraphy of the Nicola Group in the Hedley District, British Columbia, and the chemistry of its intrusions and Au Skarns; *Canadian Journal of Earth Science*, Volume 33, pages 1105-1126.
- Redwood, S.D. (1999): The geology of the Antamina copper-zinc skarn deposit, Peru; in *The Gangue*, *Geological Association of Canada*, Issue 60, pages 1-7.
- Rotzien, J. (1991): Diamond Drill Report on the MV 1 Claim; *British Columbia Ministry of Energy and Mines*, Assessment Report 21965, 61 pages.
- Rotzien, J. (1992): Diamond Drill Report on the MV 1 Claim; *British Columbia Ministry of Energy and Mines*, Assessment Report 21965, 132 pages.
- Soregaroli, A. (1999): Memo on regional geological, geochemical and geophysical studies performed in the Lustdust area by research institutions; unpublished report for *Alpha Gold Corporation*, pages.
- Schiarizza, P. (2000): Bedrock geology, Old Hogem (Western Part), NTS 93N/11, 12, 13; British Columbia Ministry of Energy and Mines, Open File 2000-33, 1:100 000 scale.
- Schiarizza, P., and MacIntyre, D. (1999): Geology of the Babine Lake-Takla Lake area, central British Columbia (93K/11, 12, 13, 14: 093N/3, 4, 5, 6); in *Geological Fieldwork 1998*, *British Columbia Ministry of Energy and Mines*, Paper 1999-1, pages 33-68.
- Sun, S.S. and McDonough, W.F. (1989): Chemical and isotopic systematics of oceanic basalts: implications for mantle composition and processes; in *Magmatism in the ocean basins*. Saunders, A.D. and Norry, M.J., Editors, *Geological Society*, Special Publication Number 42, pages 313-345.
- Sutherland Brown, A., (1965): Lustdust (Takla Silver Mines Limited), *British Columbia Ministry of Mines and Petroleum Resources*, Annual Report 1965, page 105.
- Wheeler, J.O., Brookfield, A.J., Gabrielse, H., Monger, J.W.H., Tipper, H.W. and Woodsworth, G.J. (1991): Tectonic assemblage map of the Canadian Cordillera; *Geological Survey of Canada*, Map 1712a, Scale 1:2 000,000.
- Winchester, J.A., and Floyd, P.A. (1977): Geological discrimination of different magma series and their differentiation products using immobile elements; *Chemical Geology*, Volume 20, pages 325-343.